8) Imai Y, Soda M, Inoue H, et al: An unfolded putative transmembrane polypeptide, which can lead to endoplasmic reticulum stress, is a substrate of Parkin. Cell 105: 891-902, 2001
9) Plemper RK, Wolf DH: Retrograde protein translocation: ERADication of secretory proteins in health and disease. Trends Biochem Sci 24: 266-270, 1999
10) Nakagawa T, Zhu H, Morishima N, et al: Caspase-12 mediates endoplasmic-reticulum-specific apoptosis and cytotoxicity by amyloid-beta. Nature 403: 98-103, 2000
11) Dawson TM, Dawson VL: Molecular pathways of neurodegeneration in Parkinson's disease. Science 302: 819-822, 2003
12) Honbou K, Suzuki NN, Horiuchi M, et al: The crystal structure of DJ-1, a protein related to male fertility and Parkinson's disease. J Biol Chem, in press, 2003
13) Kitada T, Asakawa S, Hattori N, et al: Mutations in the parkin gene cause autosomal recessive juvenile parkinsonism. Nature 392: 605-608, 1998
14) Lansbury PT, Brice A: Genetics of Parkinson's disease and biochemical studies of implicated gene products. Curr Opin Cell Biol 14: 653-660, 2002
15) Mizuno Y, Hattori N, Mori H, et al: Parkin and Parkinson's disease. Curr Opin Neurol 14: 477-482, 2001
16) Mori, K: Tripartite management of unfolded proteins in the endoplasmic reticulum. Cell 101: 451-454, 2000
17) Nagakubo D, Taira T, Kitaura H, et al: DJ-1, a novel oncogene with which transforms mouse NIH3T3 cells in cooperation with ras. Biochem Biophys res Commun 231: 509-513, 1997
18) Polymeropoulos MH, Lavedan C, Leroy E, et al: Mutation in the alpha-synuclein gene identified in families with Parkinson's disease. Science 276: 2045-2057, 1997
19) Sakata E, Yamaguchi Y, Kurimoto E, et al: Parkin binds the Rpn10 subunit of 26S proteasomes through its ubiquitin-like domain. EMBO Rep 4: 301-306, 2003
20) Shimura H, Hattori N, Kubo S, et al: Familial Parkinson disease gene product, parkin, is a ubiquitin-protein ligase. Nat Genet 25: 302-305, 2000
21) Shimura H, Schlossmacher MG, Hattori N, et al: (2001) Ubiquitination of a new form of alpha-synuclein by parkin from human brain: implications for Parkinson's disease. Science 293: 263-269, 2001
22) Steece-Collier K, Maries E, Kordower JH: Etiology of Parkinson's disease: Genetics and environment revisited. Proc Natl Acad Sci U S A 99: 13972-13974, 2002
23) 田中啓二：新手を繰り出すユビキチンの魔術．実験医学 21: 330-339, 2003
24) Taira T, Saito Y, Niki T, et al: DJ-1 has a role in antioxidantive stress to prevent cell death. EMBO reports 5: 213-218, 2004
25) 高橋良輔：パーキンの機能．生化学 74: 471-476, 2002
26) Valente EM, Abou-Sleiman PM, Caputo V, et al: Hereditary Early-onset Parkinson's disease caused by mutations in PINK1. Science 304: 1158-1160, 2004
27) Yang Y, Nishimura I, Imai Y, et al: Parkin suppresses dopaminergic neuron-selective neurotoxicity induced by Pael-R in Drosophila. Neuron 37: 911-924, 2003
28) Zhang Y, Gao J, Chung KK, et al: Parkin functions as an E2-dependent ubiquitin- protein ligase and promotes the degradation of the synaptic vesicle-associated protein, CDCrel-1. Proc Natl Acad Sci U S A 97: 13354-13359, 2000

ユビキチンプロテアソーム蛋白質分解系と神経変性疾患治療戦略

高橋　良輔

神経治療学　第22巻　第6号　別刷
平成17年11月25日発行
Reprinted from Neurological Therapeutics, Vol. 22, No. 6, p. 697-702, November 2005

ユビキチンプロテアソーム蛋白質分解系と神経変性疾患治療戦略*

高橋　良輔**

Key Words : protein folding, conformational disease, Parkinson's disease, ubiquitin ligase, endoplasmic reticulum

はじめに

「神経変性疾患」は原因不明の難病の代名詞であったが，分子遺伝学の著しい進歩により，この20年ほどの間に主要な遺伝性神経変性疾患の病因遺伝子があらかた同定され，その遺伝子産物である病因蛋白質の機能解析が進んだ結果，さまざまな神経変性疾患にはじつは共通の分子機構があるらしいことがかなり確かな事実として浮上してきた．「共通の分子機構」とは，すなわち構造異常を起こした蛋白質の蓄積である（**Fig. 1**）．蛋白質は本来の機能を果たすために正しい3次構造をとるために折りたたまれる（フォールディングという）ことが必要であるが，フォールディングに失敗した蛋白質（ミスフォールド蛋白質と呼ばれる）は機能を失うだけでなく，細胞にとって有害な性質を獲得し，神経変性を引き起こすらしい[1, 2]．遺伝性疾患の場合は容易に理解されるように，遺伝子変異によってアミノ酸配列が変わるために，病因蛋白質はミスフォールド化する．ところが意外なことに蛋白質のミスフォールド化はアミノ酸配列が正常でも，健康人であっても，常に生じている．これはフォールディングという過程が100%成功するプロセスではないことによっている．新しくできた蛋白質の約30%はミスフォールド化するという報告[3]は現在疑問視されているが，恒常的にミスフォールド化が生じていることは確かである．このようなミスフォールド化蛋白質は，後述のユビキチンプロテアソーム蛋白質分解系の働きによって分解処理されるので，健康人では問題を起こさない．ところが，分解系が低下すると，ミスフォールド化した蛋白質は蓄積を開始し，変異蛋白質と同じように有害な性質で神経変性を引き起こす可能性がある．これは孤発性神経変性疾患の成因を合理的に説明しうる（**Fig. 1**）．しかも孤発性神経変性疾患は加齢が唯一かつ強力なリスクファクターであるが，加齢とともにユビキチンプロテアソーム系の活性が低下することがわかっており，観察事実からも分解系低下に孤発性疾患の成因を求める考えは当を得ているように思われる．さらに加齢とともに酸化的ストレスが蓄積することもよく知られた事実であるが，酸化的ストレスは蛋白質を酸化修飾して，ミスフォールド化を促進させることも容易に想定される（**Fig. 1**）．このようにユビキチンプロテアソーム蛋白質分解系をキーワードとして考えると，遺伝性と孤発性の神経変性疾患がともにミスフォールド蛋白質の蓄積で統一的に理解できる．このような観点から，神経変性疾患は蛋白質の構

* Ubiquitin-Proteasome System and the Strategies for the Therapeutics of Neurodegenerative Diseases.

** 京都大学大学院医学研究科臨床神経学（神経内科） Ryosuke TAKAHASHI : Department of Neuology, Kyoto University Graduate School of Medicine

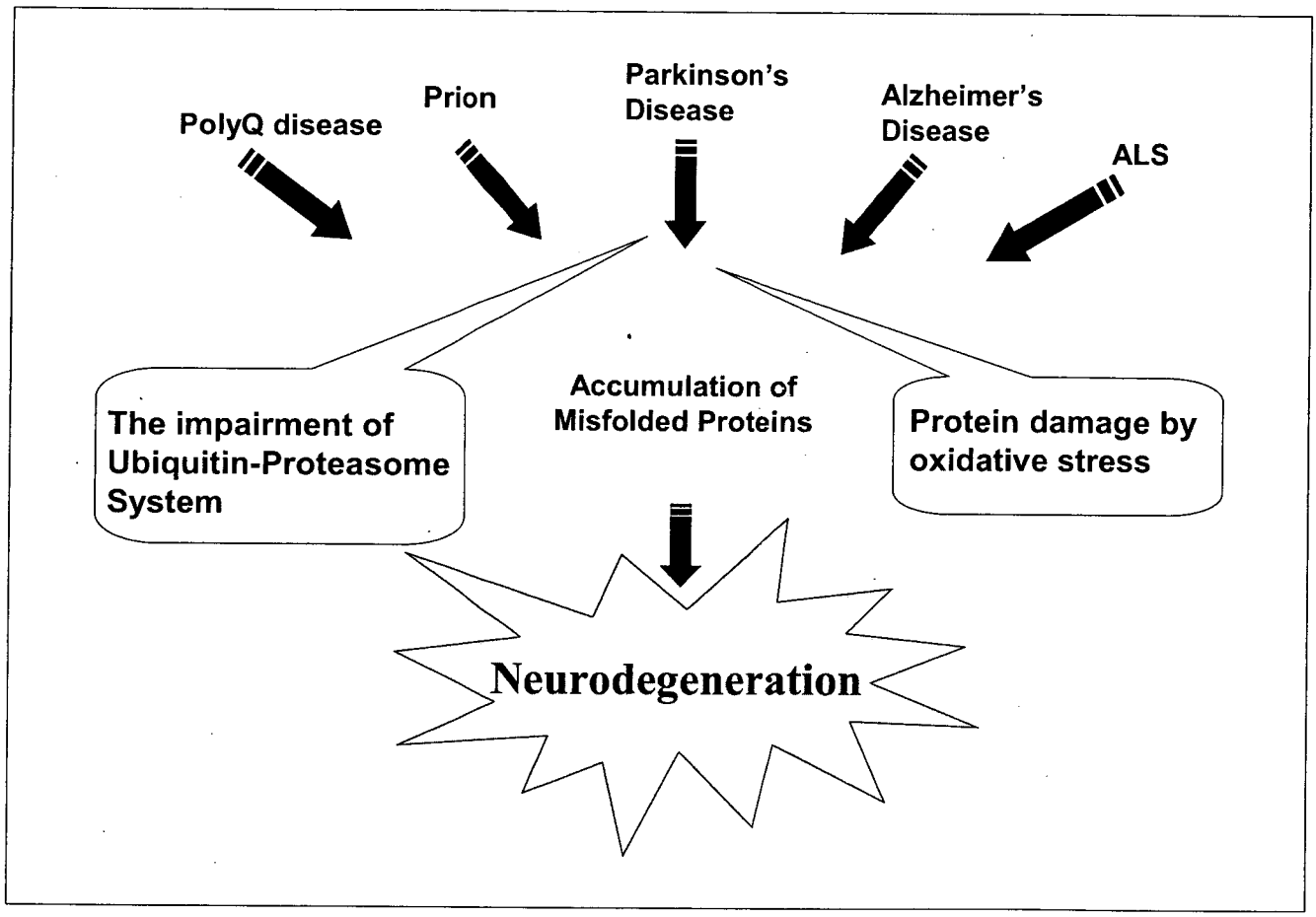

Fig. 1 Common pathogenetic mechanisms for various neurodegenerative diseases

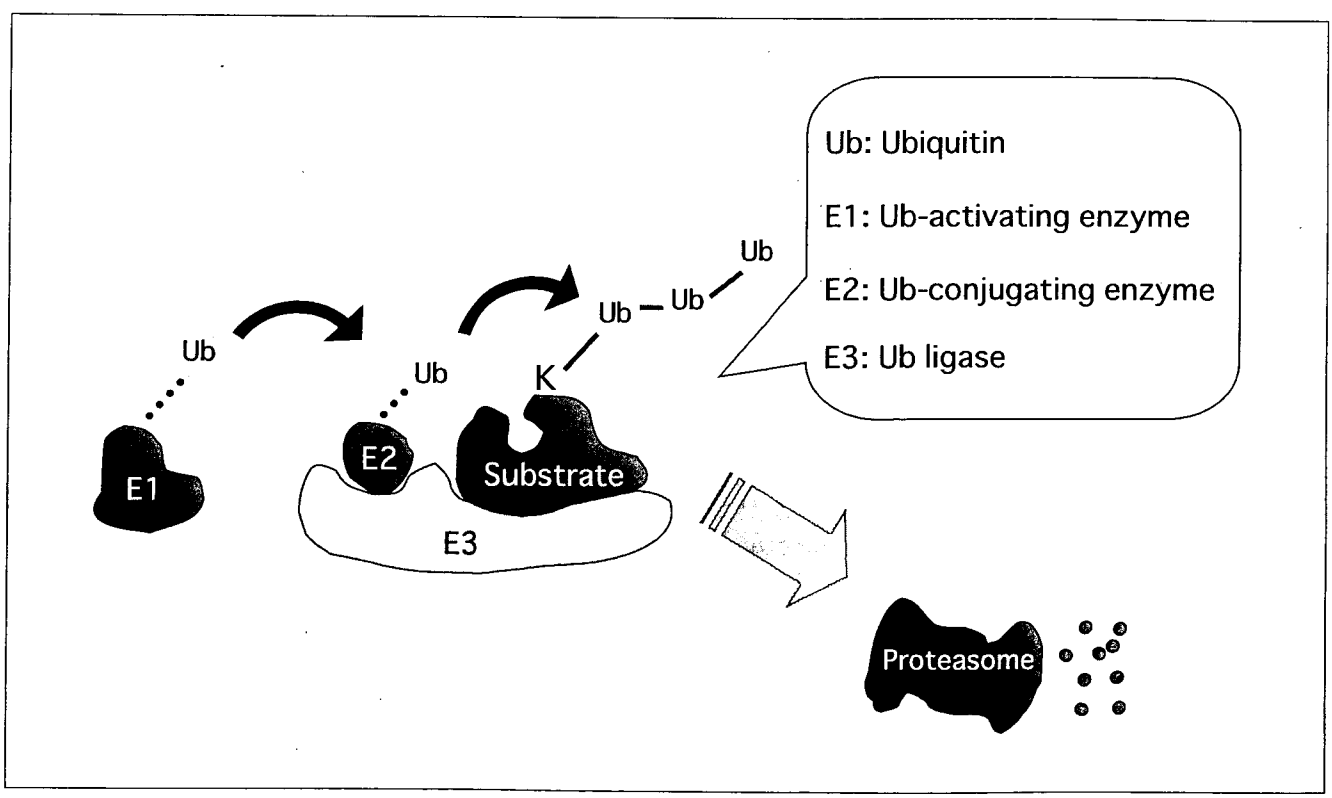

Fig. 2 Ubiquitin-proteasome system

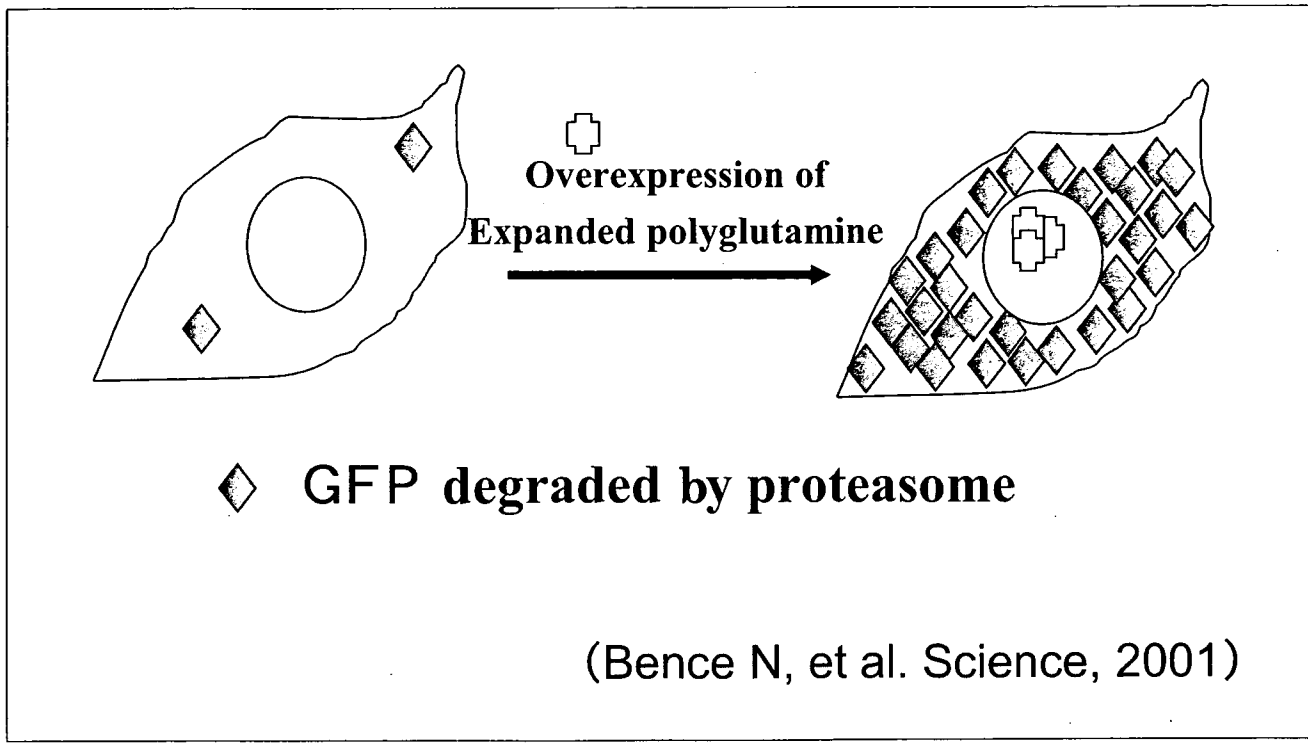

Fig. 3 Misfolded proteins inhibit proteasomal activity

造異常によって生じるという意味で，構造病（コンフォメーション病：conformational disease）の代表的な疾患と考えられるようになった[4, 5]．本稿ではParkinson病を中心としてユビキチンプロテアソーム系の神経変性疾患への関与について述べる．

I．ユビキチンプロテアソーム蛋白質分解系とは

ユビキチンプロテアソーム系（Ubiquitin-proteasome system；UPS）は細胞内のおおよそ半減期が10時間以下の短寿命の蛋白質の分解を担う主な分解系であり，分解にATPを消費するエネルギー依存性と分解する基質を選択する基質選択性をもつ2つの特徴を備えている[5]（**Fig. 2**）．ユビキチンは76アミノ酸からなる小さな蛋白質であるが，蛋白質分解の目印としての役割を果たす．ユビキチンが4つ以上鎖状につながったポリユビキチン鎖が蛋白質に共有結合すると，プロテアソームがポリユビキチン化された基質蛋白質を認識し，分解する．すなわち，蛋白質のユビキチン化が基質の選択を決定する重要なステップとなる．ユビキチン化はE1（ユビキチン活性化酵素），E2（ユビキチン結合酵素），E3（ユビキチンリガーゼ）という3種類の酵素の連続的な反応によって行われる．このうちE1はATPを使って，高エネルギーのチオールエステル結合をユビキチンとの間に形成し，それがE2に引き渡される．E3は基質を特異的に認識する重要な役割を担うが，E3の仲立ちで，ユビキチンは基質のリジン残基に安定なペプチド結合を形成する．ユビキチン化の反応は繰り返して起こるが，2番目以降のユビキチンが直前のユビキチンに結合する結果，ポリユビキチン鎖が形成される．ポリユビキチン化蛋白質は26Sプロテアソームの19Sキャップという蓋のような部分によって認識され，ここでまたATPを使ってフォールディングを解かれ，アミノ酸のひものような形になってシリンダー状の20Sプロテアソームの内腔に送り込まれ，カタリティックサブユニットの働きで分解される．このような複雑な機構を生体が用意した理由の一部には，細胞内で絶えず産生される有害なミスフォールド蛋白質を見分け，分解処理する必要があることがあげられるであろう．

II．ミスフォールド蛋白質とUPS

ところが，ミスフォールド蛋白質はUPSの基質となると同時にUPSの機能を低下させる性質があることがわかってきた．このことを示した

Ron Kopitoたちのエレガントな実験を紹介する[6] (**Fig. 3**). 彼らは本来は極めて安定なGreen Fluorescent Protein (GFP) にdegronという配列を付加し，プロテアソームで速やかに分解される不安定な蛋白質GFP^uを作製した．GFP^uを過剰発現させるとプロテアソームの活性が保たれている細胞では分解されてしまうため蛍光を発しないが，プロテアソームの活性が低下すると蛋白質が蓄積する結果，蛍光を発するようになる．すなわちGFP^uはプロテアソーム活性のセンサーの役割を果たす．GFP^uを発現する細胞にミスフォールド蛋白質の代表例であるポリユビキチンを発現させると，蛍光の観察されなかった細胞で，一転して蛍光がみられるようになり，プロテアソーム活性が低下することが示された．彼らはポリグルタミンによって核内に封入体の形成された細胞で特にプロテアソーム活性が低下していることから，ポリグルタミン凝集体がプロテアソーム活性を阻害する可能性を強く考えている．しかし凝集体を形成する細胞では凝集体形成にいたるまでのミスフォールド蛋白質も増加していると思われるので，「ポリグルタミン蛋白質がプロテアソーム活性を阻害する」ことを示す証拠ととらえるのが合理的である[7]．ほぼ同時期に貫名信行らのグループもポリグルタミンでプロテアソーム活性が阻害されると報告し[8]，Christopher Rossらのグループはα-シヌクレイン（後述）でも同様の観察をしており[9]，ミスフォールド蛋白質が一般にプロテアソーム活性を阻害する可能性が強く支持されるようになった．

ミスフォールド蛋白質がプロテアソームによって分解される一方，ミスフォールド蛋白質がプロテアソームを阻害するとすれば，ミスフォールド蛋白質の蓄積はプロテアソームの阻害を引き起こし，さらなるミスフォールド蛋白質の蓄積を招くという悪循環を経て神経変性に至るというシナリオを描くことができる．この興味深いが，やや単純化され過ぎたようにもみえるこの仮説が基本的に正しいかどうかは今後個々の疾患で確かめられる必要があるだろう．

III. 家族性Parkinson病とUPS

神経変性疾患におけるUPSの重要性に関しては，特に家族性Parkinson病において遺伝子レベルで有力な証拠が得られている．家族性Parkinson病は現在までに11種類の異なる遺伝子座にリンクする疾患が見つかっており，そのうち7疾患に関しては病因遺伝子まで単離されている．ユビキチンプロテアソーム系との関わりが示されているのは，そのうち，脱ユビキチン酵素であるUCH-L1，ユビキチンリガーゼであるParkin，そしてミスフォールド化しやすいα-シヌクレインの3種類で，それぞれ，PARK5，PARK2，PARK1の病因遺伝子である．以下ではα-シヌクレインとParkinに焦点を絞ってこれらの遺伝子変異を成因とするPARK1とPARK2のUPSとの関わりについて述べる[10, 11]．

IV. α-シヌクレインとUPS

α-シヌクレインは140アミノ酸の神経特異的な蛋白質で神経終末に豊富に存在するが，その生理的役割は不明である．α-シヌクレインの点突然変異によるミスセンス変異（A53T）で常染色体優性遺伝性Parkinson病になることが1997年明らかになり，その後2種類のミスセンス変異（A30P，E46K）が同定されたが，いずれもきわめてまれな変異で，日本人ではまだ見つかっていない．ところが，α-シヌクレインがParkinson病の病理学的特長であるLewy小体の主成分であることが判明し，Parkinson病の鍵を握る分子として一躍注目を集めるようになった．さらにα-シヌクレインを含む染色体領域の二重複，三重複（従来PARK4と呼ばれていた家系）も優性遺伝のα-シヌクレインを引き起こすことがわかり，量的に増加するだけで発症につながることが明らかになったことから，孤発性Parkinson病ではα-シヌクレインの産生亢進，または分解低下が発症に関わるという考えがにわかに説得性を帯びるようになった．事実，α-シヌクレインのトランスジェニック動物（マウス，ショウジョウバエ）では部分的にParkinson病の症状，病理所見を再現する．また，プロテアソーム阻害剤を全身的，または線条体局所に投与することによってα-シヌクレイン陽性細胞内凝集体形成を伴う黒質ドーパミン神経の変性が起こり，UPSの活性低下がParkinson病発症に結びつくという考えを裏付け

ている．最近，α-シヌクレインはUPSのみならずリソソーム系，またはシャペロン介在性オートファジーによって分解されるとの証拠も提出されているので，オートファジーとParkinson病の関係も今後注目される．

V. ParkinとUPS

ParkinはPARK2，または常染色体劣性若年性パーキンソニズム（AR-JP）の病因遺伝子であるが，UPSで重要な役割を果たすユビキチンリガーゼ（E3）である．E3は前述のように基質蛋白質を特異的に認識する役割を担っていることから，Parkinの変異でE3活性が失われた結果基質蛋白質が蓄積するのがAR-JPの発症メカニズムであると考えられるようになった．現在までに10種類以上のParkinの基質候補が見つかっているが，そのうち，蓄積による細胞死を最も明解に説明できる基質蛋白質が，われわれが同定したミスフォールド化パエル受容体（Pael-R）である．Pael-Rはリガンド不明のG蛋白質共役型受容体である[12]．Pael-Rを含めた新生膜蛋白質は小胞体でシャペロンの助けでフォールディングされる．正しい構造を取れた蛋白質は膜に送り込まれるが，フォールディングに失敗し，ミスフォールド化した，いわばごみになった蛋白質は細胞質に再輸送されて，そこでUPSによって分解される．この膜蛋白質のごみ処理分解経路のことを小胞体関連分解（Endoplasmic Reticulum-Associated Degradation；ERAD）と呼んでいるが，われわれはミスフォールド化Pael-RがERADにおいてParkinによってユビキチン化され，分解処理されることを突き止めた．ParkinのE3活性が失われると，ミスフォールド化Pael-Rは小胞体に蓄積して，小胞体ストレスを引き起こし，そのストレス応答の結果細胞死が起こるものと思われる．この考えに一致して，ショウジョウバエ，またはマウスでPael-Rを過剰発現するとドーパミンニューロンの変性脱落が観察される．Parkinノックアウトマウスではpael-Rを含めて既知の基質蛋白質の蓄積はみられず，ドーパミン神経細胞死も起こらない．この事実は基質の蓄積でAR-JPのメカニズムを説明できるかという根源的な疑問を生み出しているが，別の観点からは現在は困難である不溶性蛋白質のわずかな量的変化を検出することが技術的に可能になれば，新しい証拠が得られる可能性がある．

おわりに

現在神経変性疾患の進行をとめたり，発症を予防するような有効な治療法は知られていないが，ここで述べてきたようなUPSとの関連で考えると，異常蛋白質の産生を抑制したり，あるいはその分解系を賦活化する治療法，あるいはミスフォールド化蛋白質がUPSを阻害する過程を抑制するような治療法が考えられる．またミスフォールド化蛋白質による神経変性誘発機構をより正確に理解することが，新しい治療法の確立に重要であろう．

文　献

1）Taylor JP, Hardy J, Fischbeck KH : Toxic proteins in neurodegenerative disease. Science 296 : 1991-1995, 2002
2）Kopito RR : Aggresomes, inclusion bodies and protein aggregation. Trends Cell Biol 10 : 524-530, 2000
3）Schubert U, Anton LC, Gibbs J et al : Rapid degradation of a large fraction of newly synthesized proteins by proteasomes. Nature 404 : 770-774, 2000
4）Carrell RW, Lomas DA : Conformational disease. Lancet 350 : 134-138, 1997
5）Hershko A, Ciechanover A : The ubiquitin system. Annu Rev Biochem 67 : 425-479, 1998
6）Bence NF, Sampat RM, Kopito RR : Impairment of the ubiquitin-proteasome system by protein aggregation. Science 292 : 1552-1555, 2001
7）Bennett EJ, Bence NF, Jayakumar R et al : Global impairment of the ubiquitin-proteasome system by nuclear or cytoplasmic protein aggregates precedes inclusion body formation. Mol Cell 17 : 351-365, 2005
8）Jana NR, Zemskov EA, Wang G et al : Altered proteasomal function due to the expression of polyglutamine-expanded truncated N-terminal huntingtin induces apoptosis by caspase activation through mitochondrial cytochrome c release. Hum Mol Genet 10 : 1049-1059, 2001
9）Tanaka Y, Engelender S, Igarashi S et al : Inducible expression of mutant alpha-synuclein decreases proteasome activity and increases sensi-

tivity to mitochondria-dependent apoptosis. Hum Mol Genet 10 : 919-926, 2001
10) Cookson MR : The biochemistry of Parkinson's disease. Annu Rev Biochem 74 : 29-52, 2005
11) Moore DJ, West AB, Dawson VL et al : Molecular pathophysiology of Parkinson's disease. Annu Rev Neurosci 28 : 57-87, 2005
12) Takahashi R, Imai Y, Hattori N et al : Parkin and endoplasmic reticulum stress. Ann N Y Acad Sci 991 : 101-106, 2003

Ubiquitin-Proteasome System and the Strategies for the Therapeutics of Neurodegenerative Diseases

Ryosuke TAKAHASHI

Department of Neuology, Kyoto University Graduate School of Medicine

A growing body of evidence strongly suggests that accumulation of misfolded proteins constitutes the common pathogenetic mechanisms underlying various neurodegenerative disorders. Since ubiquitin-proteasome protein degradation system (UPS) plays a principal role in the degradation of cellular misfolded proteins, the impairment of UPS associated with aging may lead to development of sporadic neurodegenerative diseases. Moreover, mifolded proteins inhibit proteasomal activity when over expressed in the cell. Based on these lines of data, accumulation of misfolded protein and proteasomal impaiment form a vicious cycle, leading to a catastrophic neurodegeneration and neuronal death. Familial Parkinson' diseases (PD) provide excellent examples for the involvement of UPS in Parkinson' s disease. Missense mutaions and gene multiplication mutations of α-synuclein, a neuron-specific presynaptic protein, are responsible for PARK1, an autosomal dominant form of familial PD. α-synuclein turned out to be a major component of Lewy body, suggesting that accumulation of α-synuclein leads not only to familial forms but sporadic form of PD. Systemic or local striatal inhibiton of proteasome induced dopaminergic cell loss accompanied by α-synuclein-positive intracellular aggregates, providing evidence that proteasomal impairment may be causative in sporadic PD. Parkin is the gene responsible for autosomal recessive familial parkinsonism (AR-JP), or PARK2. Parkin turned out to be a ubiquitin ligase, which specifically recognizes substrate protein (s), ubiquitinate them to promote their degradation. Among 10 different Parkin substrates, misfolded Pael-R is one of the best characterized one. Misfolded Pael-R is ubiquitinated with the help of Parkin in the endoplasmic reticulum (ER)-associated degradation (ERAD) pathway. When Parkin is mutated, misfolded Pael-R accumulates in the ER, leading to ER stress-induced apoptosis. Pael-R induced dopaminergic cell death is recapitulated in transgenic Drosophila and mice. Based on these findings, future therapeutics against intractable neurodegenerative diseases should include downregulation of the causative misfolded proteins and/or enhancement of UPS.

nature neuroscience

Chromogranin-mediated secretion of mutant superoxide dismutase proteins linked to amyotrophic lateral sclerosis

Makoto Urushitani[1], Attila Sik[2], Takashi Sakurai[3], Nobuyuki Nukina[3], Ryosuke Takahashi[4] & Jean-Pierre Julien[1]

Here we report that chromogranins, components of neurosecretory vesicles, interact with mutant forms of superoxide dismutase (SOD1) that are linked to amyotrophic lateral sclerosis (ALS), but not with wild-type SOD1. This interaction was confirmed by yeast two-hybrid screen and by co-immunoprecipitation assays using either lysates from Neuro2a cells coexpressing chromogranins and SOD1 mutants or lysates from spinal cord of ALS mice. Confocal and immunoelectron microscopy revealed a partial colocalization of mutant SOD1 with chromogranins in spinal cord of ALS mice. Mutant SOD1 was also found in immuno-isolated trans-Golgi network and in microsome preparations, suggesting that it can be secreted. Indeed we report evidence that chromogranins may act as chaperone-like proteins to promote secretion of SOD1 mutants. From these results, and our finding that extracellular mutant SOD1 can trigger microgliosis and neuronal death, we propose a new ALS pathogenic model based on the toxicity of secreted SOD1 mutants.

ALS is a progressive adult-onset neurodegenerative disorder that affects primarily motor neurons in the brain and spinal cord. The disease typically begins locally and spreads, leading to paralysis and death within 3–5 years. Approximately 10% of ALS cases are familial and 90% are sporadic. Mutations in the genes encoding SOD1 (ref. 1) are involved in 20% of familial ALS cases.

Despite a decade of investigation on familial ALS caused by missense mutations in the *SOD1* gene, the mechanism of toxicity to motor neurons has remained elusive. Transgenic mice expressing mutant forms of SOD1 develop motor neuron disease resembling ALS through a gain of unidentified deleterious properties[2]. Eliminating the copper chaperone for SOD1 does not diminish the toxicity of mutant SOD1 in mice[3], and mutations that disrupt the copper-binding site of mutant SOD1 do not suppress toxicity[4]. Thus, it is now thought that the toxicity of mutant SOD1 is not related to aberrant copper-mediated catalysis but rather to the propensity of the abnormal protein to aggregate, a phenomenon common to many neurodegenerative diseases[5,6]. Cell culture studies have shown that the mutant SOD1 proteins induce oxidative stress[7,8], form aggregates[9,10] and impair proteasomal function[11].

Notably, recent lines of evidence indicate that the toxicity of SOD1 mutants is non-cell-autonomous. The neuron-specific expression of mutant SOD1 does not provoke motor neuron disease[12,13]. Moreover, chimeric mouse studies with SOD1 mutants have demonstrated that neurodegeneration is delayed or eliminated when motor neurons expressing mutant SOD1 are surrounded by healthy wild-type cells[14]. Moreover, these studies show evidence of damage to wild-type motor neurons by surrounding cells expressing mutant SOD1. Such results emphasize the importance of a motor neuron milieu, but the mechanism by which the toxicity of mutant SOD1 may be transferred from one cell to another is still unclear[14].

So far, proteins known to interact with mutant forms of SOD1 but not with wild-type SOD1 have been implicated in protein refolding or proteasomal degradation (for example, heat-shock proteins Hsp40, Hsp/Hsc70 (refs. 15,16) and CHIP[16]). To search for more proteins that interact with mutant SOD1, we performed yeast two-hybrid screening of a cDNA library from the total spinal cord of presymptomatic transgenic mice expressing the G93A SOD1 mutation (in which a glycine residue is replaced by an alanine residue). We discovered that chromogranins are interacting partners with mutant forms of SOD1, but not wild-type SOD1. The chromogranins, namely chromogranin-A (CgA) and chromogranin-B (CgB), are soluble, acidic glycophosphoproteins and are major constituents of secretory large dense-core vesicles (LDCV) in neurons and endocrine cells. LDCV store neuropeptides and hormones and show regulated exocytosis upon appropriate cellular stimulation[17]. Chromogranins are transported in the trans-Golgi network (TGN) and translocate at the periphery in an actin-dependent manner during their maturation process[18]. Although the physiological functions of chromogranins are still unclear, previous reports have shown that their proteolytic products function as antibiotics, regulators of hormone release, controllers of intracellular Ca^{2+} concentration and protein sorting machineries[17]. The role of chromogranins in neurons is unknown. Both CgA and CgB proteins are transported in the rat sciatic

[1]Department of Anatomy and Physiology, Laval University, Centre de Recherche du Centre Hospitalier de l' Université Laval, 2705 boulevard Laurier, Sainte-Foy, Quebec G1V 4G2, Canada. [2]Department of Psychiatry, Centre de Recherche Université Laval Robert-Giffard, 2601 de la Canardiere, Quebec, Quebec G1J 2G3, Canada. [3]Laboratory for Structural Neuropathology and [4]Motor System Neurodegeneration, RIKEN Brain Science Institute, 2-1 Hirosawa, Wako, Saitama, 351-0198, Japan. Correspondence should be addressed to J.-P.J. (jean-pierre.julien@crchul.ulaval.ca).

Received 15 September; accepted 26 October; published online 20 December 2005; doi:10.1038/nn1603

nerve[19] and CgA is found in motor endplates in the diaphragm[20], suggesting a possible role in neurotransmission.

Previous evidence indicates that chromogranins are involved in neurodegenerative diseases. Immunohistochemical studies have revealed the presence of CgA or CgB in neuritic senile plaques of Alzheimer brains[21] and in prion protein deposits of Creutzfeldt-Jacob disease brains[22]. The staining pattern of CgA is also altered in motor neurons of people with sporadic ALS[23]. Importantly, there is evidence that CgA can activate microglia to produce various pro-inflammatory molecules such as tumor necrosis factor-alpha (TNF-α), nitric oxide and potential neurotoxins including glutamate and cathepsin B[24–26].

Here we report that CgA and CgB, which are abundant proteins in motor neurons and interneurons, may act as chaperone-like proteins to

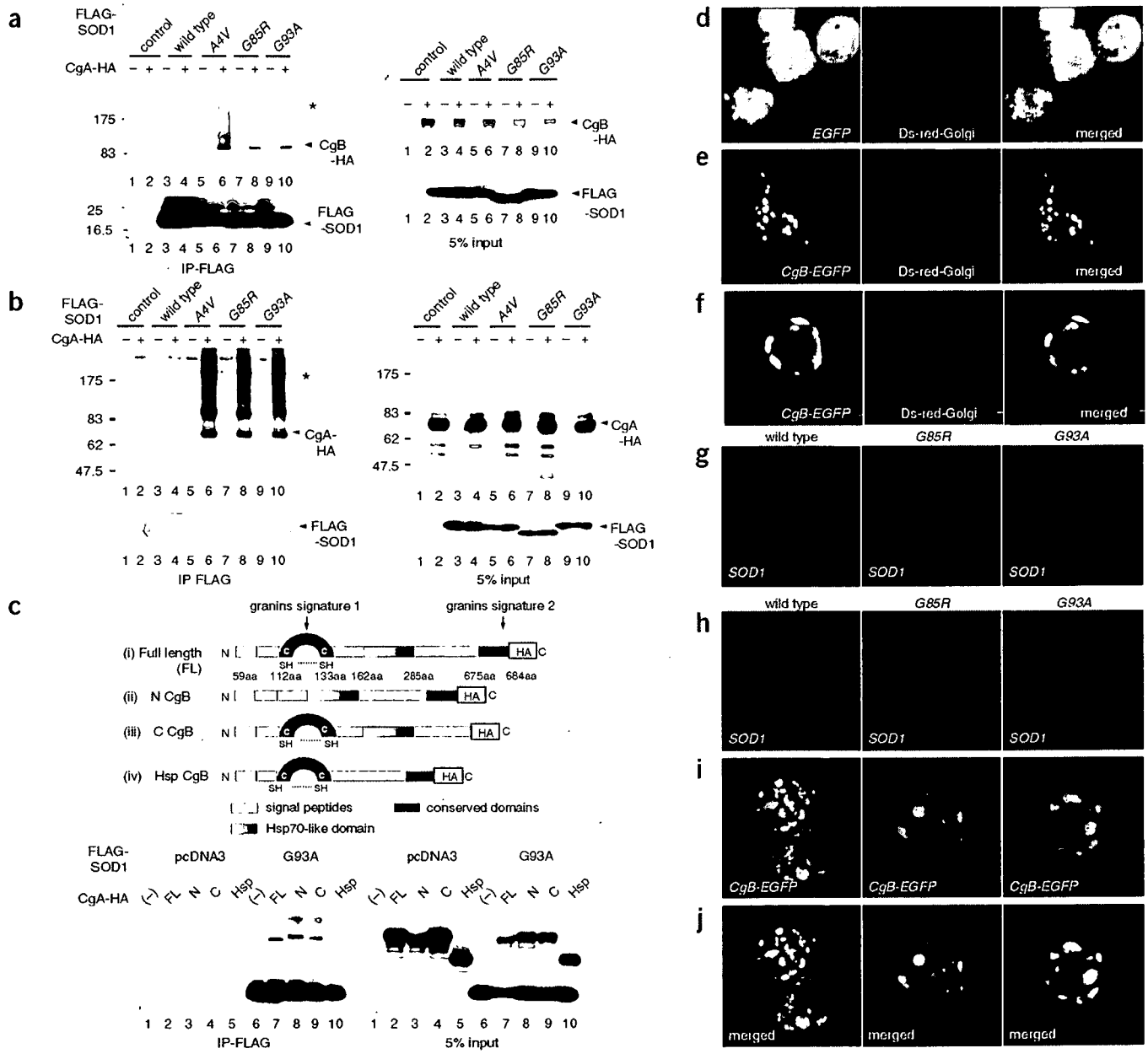

Figure 1 Selective interactions of chromogranins with mutant SOD1 species but not with wild-type SOD1. (**a**,**b**) Chromogranins interact with mutant SOD1 in cultured cells. Neuro2a cells were transiently transfected with FLAG-tagged human *SOD1* (wild-type, A4V, G85R or G93A) and HA-tagged mouse CgB (**a**) or CgA (**b**). Immunoprecipitates with anti-FLAG affinity gel (IP-FLAG) and total cell lysates (5% input) were analyzed by western blotting using antibodies to SOD1 or HA. Note that both CgB and CgA immunoprecipitated with mutant SOD1 to yield high molecular weight species (asterisk). (**c**) An Hsp70-like domain in CgB interacts with mutant SOD1. Schematic representation of full-length (FL) or deletion mutants (N terminus (ΔN), C terminus (ΔC) or Hsp70-like domain (ΔHsp)) of CgB (top). Total cell lysates and immunoprecipitates from Neuro2a cells transfected with *FLAG-SOD1* or full-length *CgB* (FL) or its deletion mutants (ΔN, ΔC, ΔHsp) were analyzed by western blotting using the same antibodies (bottom). (**d–f**) Localization of CgB in the TGN of transfected Neuro2a cells. Images show live cells from confocal laser microscope of Neuro2a cells transfected with a plasmid encoding Ds-Red and a Golgi marker (*Ds-Red-Golgi*, middle) and EGFP (**d**) or EGFP-fused CgB (*CgB-EGFP*, **e** and **f**). (**g–j**) Overexpressed SOD1 mutants localized with CgB in the TGN of Neuro2a cells. Neuro2a cells were transiently transfected with human SOD1 (wild-type, G85R and G93A) together with (**i–k**) or without (**h**) CgB-EGFP, and analyzed by immunocytochemistry using mouse monoclonal anti-SOD1.

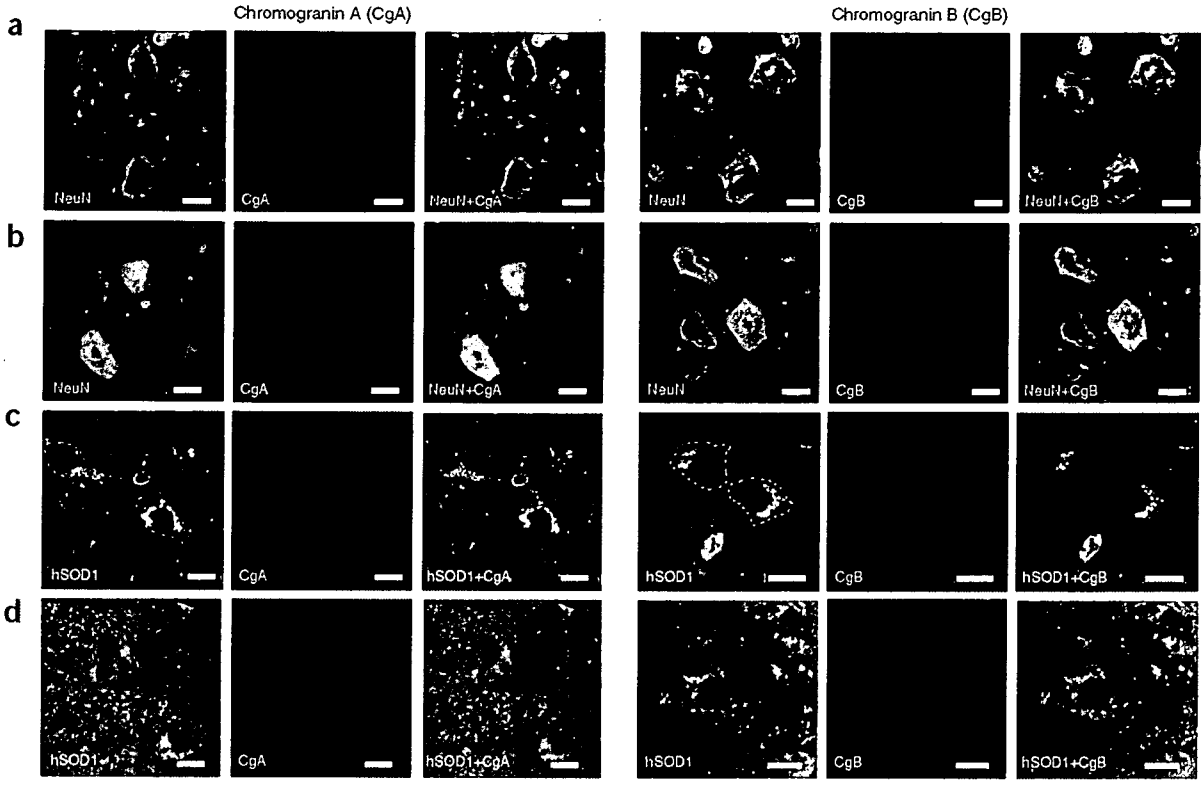

Figure 2 Expression pattern of chromogranins in *SOD1* transgenic mice. We used the lumbar spinal cords from (**a**) nontransgenic littermates, (**b**,**c**) transgenic mice at 7 months of age and (**d**) transgenic mice at 9 months of age. The transgenic mice expressed either G37R *SOD1* (**b**,**c**) or wild-type *SOD1* (**d**). The following combinations of antibody stains were used: (**a**,**b**) mouse monoclonal anti-NeuN plus rabbit polyclonal anti-CgA (left) or anti-CgB (right); (**c**,**d**) sheep polyclonal antibody specific to human SOD1 plus anti-CgA (left) or anti-CgB (right). In **c**, the dotted lines demarcate the cell body of motor neurons. Scale bars, 50 μm.

promote secretion of misfolded SOD1 mutants. Moreover, our results demonstrate that extracellular mutant SOD1 can induce microgliosis and motor neuron death, suggesting that the chromogranin-mediated secretion of mutant SOD1 proteins could be a pathogenic mechanism in ALS. This idea is consistent with findings that the disease is not strictly autonomous to motor neurons and that toxicity is transferable from one cell to another.

RESULTS

Interaction of CgA and CgB with mutant SOD1 in cultured cells

To identify new proteins that interact with mutant SOD1, we used a yeast two-hybrid approach to screen a cDNA library from the spinal cord of pre-symptomatic mice transgenic for human G93A *SOD1*, using monomeric LexA-human G93A SOD1 as bait. As expected, the majority of the 250 surviving clones expressed human SOD1 that can dimerize with the bait. However, we obtained one clone whose sequence corresponded to a partial mouse CgB sequence encoding 76 amino acids. A full-length mouse CgB clone was then isolated from a brain cDNA library of C57Bl/6 mice and used as bait in the yeast two-hybrid system to confirm a specific interaction of CgB with mutant SOD1, but not with wild-type SOD1 (data not shown). To further investigate the interaction of CgB with mutant forms of SOD1 in a mammalian cell system, we carried out transient coexpression assays with Neuro2a cells using plasmid vectors coding for CgB tagged with hemagglutinin (HA) at the carboxy (C) terminus and for various human SOD1 species tagged with FLAG at the amino (N) terminus. We tested various SOD1 mutants, including the A4V, G85R and G93A mutants, to confirm that chromogranins interact with misfolded SOD1 mutants in general, not just the G93A mutant. As shown in pull-down assays (**Fig. 1a**), CgB was co-immunoprecipitated with mutant forms of SOD1, but not with wild-type SOD1. Pull-down assays revealed that CgA, another member of the mouse chromogranin family, also associated with SOD1 mutants but not with wild-type SOD1 (**Fig. 1b**). Similar results were obtained with human chromogranins (data not shown).

CgA and CgB share two conserved domains near their N and C termini, named the granin domains. The N-terminal granin domain is implicated in a sorting mechanism[27], whereas the C-terminal granin domain is necessary for dimerization or tetramerization of chromogranins[28]. To determine the CgB region responsible for interaction with mutant SOD1, we constructed expression plasmids for CgB mutants lacking specific domains and transiently expressed them together with mutant SOD1 into Neuro2a cells (**Fig. 1c**, top). An immunoprecipitation experiment showed that CgB mutants with deleted granin domains (ΔN or ΔC) were still able to interact with mutant SOD1 (**Fig. 1c**, bottom). A search for sequence homologies revealed that both CgB and CgA contain internal sequences with homologies to the substrate-binding site of mammalian Hsp70 (**Supplementary Fig. 1** online). A CgB mutant lacking this internal region (ΔHsp) did not bind mutant SOD1, as determined by the pull-down assay (**Fig. 1c**). The presence of an Hsp70-like domain offers a reasonable explanation for the specific binding of chromogranins to misfolded SOD1 mutants and not to wild-type SOD1.

Confocal microscopy of transfected Neuro2a cells provided further evidence of interactions between SOD1 mutants and chromogranins. Transfection of a construct encoding CgB fused at the C terminus to

enhanced green fluorescent protein (EGFP) (*CgB-EGFP*) into Neuro2a cells showed CgB accumulation in the TGN, as indicated by colocalization with Ds-Red fused to the Golgi-targeting human β1,4-galactoysltransferase (Ds-Red-Golgi) (**Fig. 1d–f**). Unlike chromogranins, SOD1 is a cytosolic protein without signal peptide and it is synthesized in free ribosomes. As expected, wild-type SOD1 yielded a cytosolic distribution when overexpressed in Neuro2a cells, and the expression of CgB had no effect on its distribution (**Fig. 1g–j**, left). In contrast, the subcellular distribution of mutant SOD1 species (G85R or G93A) was altered by the overexpression of CgB. A total colocalization of mutant SOD1 with CgB was observed in roughly 10% of doubly transfected Neuro2a cells (**Fig. 1g–j**, middle and right). These results indicate that CgB can influence the subcellular distribution of SOD1 mutants under the condition of overexpression in cultured cells.

Colocalization of mutant SOD1 and CgA/B *in vivo*

We confirmed by *in situ* hybridization that CgA and CgB are expressed throughout the gray matter of spinal cord in mice, in motor neurons, interneurons and dorsal neurons. Immunohistochemistry showed that both CgA and CgB are more predominantly detected in dorsal neurons and interneurons than in motor neurons (**Supplementary Fig. 2** online), which is consistent with previous reports[29,30].

Immunofluorescence microscopy showed that CgA and CgB are located in perinuclear vesicles in the spinal motor neurons of normal mice stained by anti-NeuN antibody (**Fig. 2a**). In presymptomatic *G37R SOD1* mice (7 months old), perinuclear vesicles labeled by antibody to CgA or CgB were deformed and fused together (**Fig. 2b**), possibly reflecting damage to the Golgi apparatus[31]. We also detected partial colocalization of mutant SOD1 with CgA and CgB in irregular and large vesicular structures of spinal neurons from *G37R SOD1* transgenic mice (**Fig. 2c**). In the *SOD1* (wild-type) transgenic mice, the distribution patterns of CgA and CgB were similar to those of nontransgenic mice with no obvious colocalization between wild-type SOD1 and chromogranins (**Fig. 2d**).

To confirm the distribution of mutant SOD1 in the endoplasmic reticulum (ER)-Golgi system, we carried out subcellular fractionation of spinal cord lysates from transgenic mice expressing wild-type SOD1 or G37R SOD1 at different ages. Western blot analysis clearly demonstrated that mutant SOD1 was recovered in both heavy and light membrane fractions containing mitochondria and microsomes (**Fig. 3a**). The calculation from the densitometric value of SOD1 monomer revealed that, in the preclinical stage (6 months old), 23.6% of G37R SOD1 was found in heavy membrane fractions, and 4.2% in light membrane fractions. For wild-type SOD1, 13.4% was found in heavy membrane fractions and 1.91% in light membrane fractions. After paralysis, 6.46% of monomeric G37R SOD1 accumulated in the light membrane

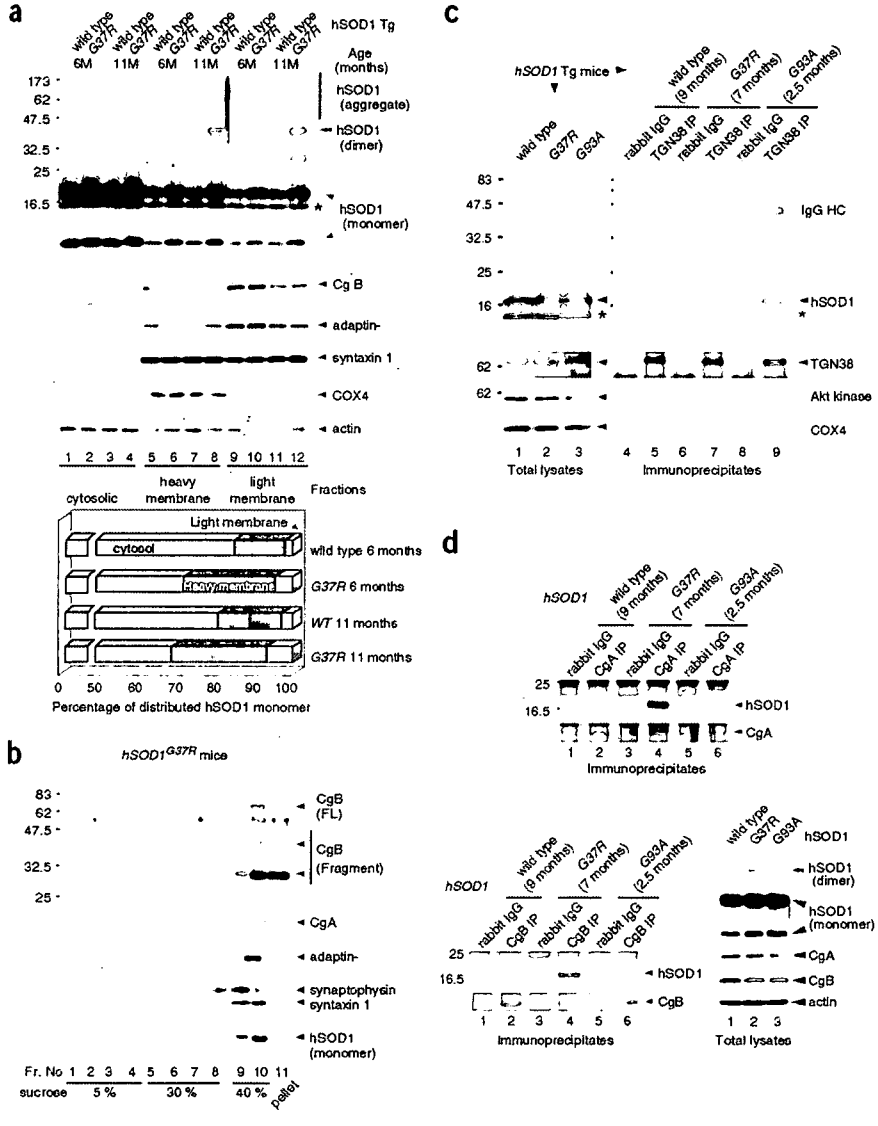

Figure 3 SOD1 mutants in spinal cord of ALS mice accumulate in TGN and co-immunoprecipitate with chromogranins. (**a**) G37R SOD1 accumulated in both heavy and light membrane fractions. Subcellularly fractionated proteins from spinal cord of wild-type and G37R *SOD1* transgenic mice (6 and 11 months old) was analyzed by western blotting using antibodies specific to human SOD1, CgB, adaptin-γ, syntaxin-1, COX4 and actin. Asterisk indicates endogenous mouse SOD1. The percentage of monomeric human SOD1 in each fraction was presented from the densitometric value of monomeric SOD1 in the cytosolic, heavy and light membrane fractions that was standardized by actin, COX4 and syntaxin-1, respectively (bottom). (**b**) Fractionation of microsome components by sucrose density-gradient ultracentrifugation showing that G37R SOD1 co-distributed with CgA, CgB, adaptin-γ and syntaxin-1. The light membrane fraction from spinal cord of G37R *SOD1* transgenic mice (7 months old) was analyzed. (**c**) Distribution of SOD1 mutants in the TGN. The spinal cord lysates from transgenic mice expressing human wild-type *SOD1* (9 months), G37R (7 months) or G93A (3 months) *SOD1* were immunoprecipitated with rabbit polyclonal anti-TGN38 preincubated with Protein G magnetic beads. The total tissue lysates and immunoprecipitates were analyzed by western blotting with antibodies to human SOD1, TGN38, Akt kinase and COX4. (**d**) Pull-down assay showing that CgA and CgB interacted with mutant SOD1 but not wild-type SOD1 in human SOD1 transgenic mice (wild-type, G37R and G93A). Spinal cord lysates were immunoprecipitated with anti-CgA or anti-CgB, which was analyzed using antibody to human SOD1.

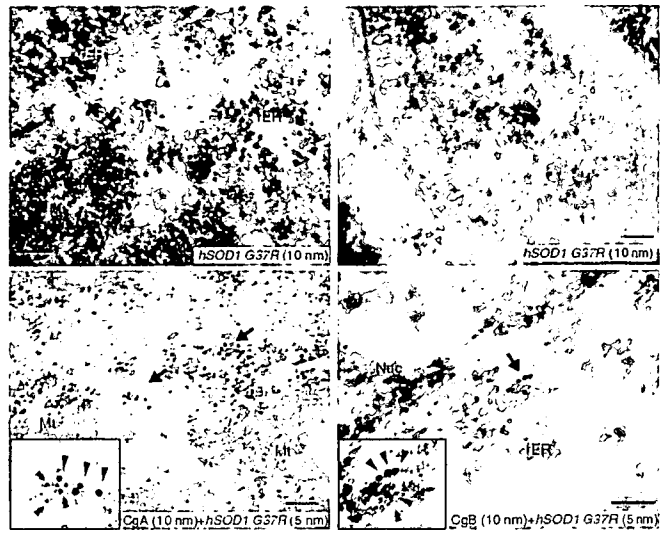

Figure 4 Immunoelectron microscopy reveals partial colocalization of G37R SOD1 with chromogranins. Ultra-thin sections of spinal anterior horn from G37R *SOD1* mice (7 months old) were incubated with sheep polyclonal antibody to human SOD1 alone (top panels), or together with rabbit polyclonal antibody to CgA or CgB (lower left or right, respectively). For secondary antibody, we used 10-nm (top panels) or 5-nm (bottom panels) immunogold-conjugated anti-sheep IgG and 10-nm immunogold-conjugated anti-rabbit IgG antibodies. In rough ER, 10-nm clusters of immuno-gold particles were frequently detected (arrowheads). G37R SOD1 was occasionally detected in mitochondria (arrow, top-left), or in a vesicle (arrowhead, top-right) close to the plasma membrane (arrows, top-right). Double-staining revealed frequent 10-nm clusters of CgA or CgB (arrowheads, bottom left or right) and 5-nm gold particles (hSOD1, double arrowheads, bottom panels). Scale bars, 100 nm.

fractions, whereas only 2.61% of wild-type SOD1 accumulated there (**Fig. 3a**, bottom). Furthermore, G37R SOD1 but not wild-type SOD1 formed non-native dimers and high molecular aggregates in the membrane fractions in an age-dependent manner. To further clarify the distribution of mutant SOD1 in the transport vesicles, we performed sucrose density gradient ultracentrifugation of post-mitochondrial membrane fractions using spinal cord extract from presymptomatic G37R *SOD1* transgenic mice at 7 months old. Western blotting revealed that mutant SOD1 had a distribution pattern similar to chromogranins, the trans-Golgi marker adaptin-γ and the SNARE protein syntaxin-1, but different from the pattern of synaptophysin (**Fig. 3b**).

To further confirm the distribution of mutant SOD1 species in a secretory pathway, we purified TGN from the spinal cord lysates of *SOD1* (wild-type), G37R *SOD1* and G93A *SOD1* transgenic mice by an immuno-isolation technique using anti-TGN38 antibody bound to protein G–coated magnetic beads. Anti-TGN38 is an affinity-purified polyclonal antibody specific to a 23-amino acid peptide corresponding to the cytosolic domain of rat and mouse TGN38 protein. Western analysis of the immunoprecipitates demonstrated that both G37R and G93A SOD1 co-precipitated with TGN38, indicating that mutant SOD1 is distributed in the TGN (**Fig. 3c**). Note that the wild-type SOD1 was also detectable in the TGN preparation, albeit at lower levels than mutant SOD1.

Further evidence for the specific interaction of CgA or CgB with mutant SOD1 proteins came from co-immunoprecipitation experiments using spinal cord lysates of transgenic mice. We found that rabbit polyclonal anti-CgA or anti-CgB antibody was able to pull down both G37R and G93A SOD1 mutants but not wild-type SOD1 (**Fig. 3d**). It should be noted that a non-native dimer of G37R SOD1 was more apparent than G93A SOD1 (double arrowhead), corresponding to the larger amount of co-immunoprecipitated G37R SOD1 than G93A SOD1.

To further investigate the distribution and colocalization of mutant SOD1 and chromogranins, we examined spinal cord sections from *SOD1* (wild-type) and G37R *SOD1* transgenic mice (7 months old) using immunoelectron microscopy. Mutant SOD1 protein was observed as small clusters of gold particles in the cytosol (**Supplementary Fig. 3** online), rough ER (arrowheads in **Fig. 4**, top-left), smooth ER and Golgi (**Supplementary Fig. 3**), and occasionally it was observed in mitochondria (arrow in **Fig. 4**, top-left) and transport vesicles (**Fig. 4**, top-right). Moreover, the double immunohistochemistry using secondary antibodies conjugated with different gold particles (5 nm or 10 nm) provided frequent detection of cluster complexes

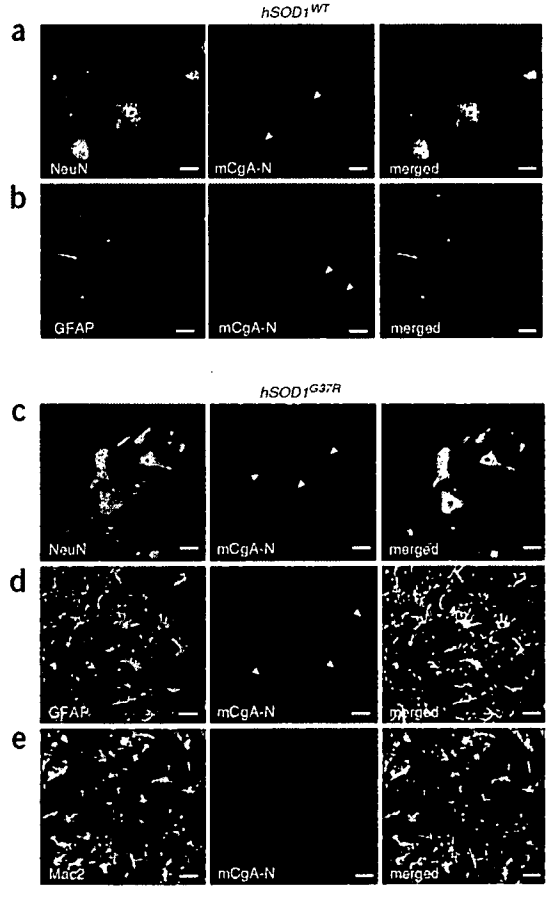

Figure 5 CgA is expressed in reactive astrocytes of spinal anterior horn from mutant *SOD1* transgenic mice. Double immunofluorescent experiments show the colocalization of CgA and GFAP in the spinal cord of transgenic mice carrying mutant *SOD1*, but not those carrying wild-type *SOD1*. (**a**,**b**) In wild-type *SOD1* mice, CgA was expressed only in the neurons labeled by anti-NeuN (**a**, mouse monoclonal), but not in reactive astrocytes labeled by anti-GFAP (**b**, mouse monoclonal). In G37R *SOD1* mice, in addition to the neuronal expression (**c**), CgA was also detected in reactive astrocytes (**d**), but not in the active microglial cells labeled by anti-Mac2 (**e**, rat monoclonal). Arrowheads and arrows, respectively, indicate neurons and astrocytes stained with anti-mCgA-N′. Left panels represent merged images from left and middle panels. Scale bars, 50 μm. Images show a representative sample from one of at least three independent experiments.

comprising SOD1 and chromogranins (**Fig. 4**; CgA bottom left, CgB bottom right). This colocalization was observed in rough ER, transport vesicles and granule-like structures. In contrast, wild-type SOD1 was chiefly located in the cytosol and occasionally in mitochondria and luminal structures including smooth and rough ER. The gold particles for wild-type human SOD1 tended to be singular or doublets, whereas clusters for G37R SOD comprised five to ten gold particles (**Supplementary Fig. 3**). No significant colocalization of wild-type SOD1 and chromogranins was detected. These findings confirm that mutant SOD1 can be recruited into the ER-Golgi pathway and interact with chromogranins.

Expression of CgA in reactive astrocytes in ALS mice

CgA is implicated in several neurodegenerative diseases including Alzheimer disease[21] and prion disease[22]. The N-terminal bioactive peptide of CgA, vasostatin, is implicated in microglial activation[24,32]. To investigate the distribution of proinflammatory fragments of CgA in the mutant *SOD1* transgenic mice, we raised a rabbit polyclonal antibody specific to the N-terminal peptide (16 amino acids) of the mature mouse CgA (anti-mCgA-N′).

Western analysis showed that anti-mCgA-N′ specifically recognized mouse CgA tagged by HA in the transfected COS-7 cells. Moreover, this antibody reacts with mouse CgA, but not with human CgA (**Supplementary Fig. 4** online). In transgenic mice overexpressing wild-type SOD1 (9 months old), immunofluorescence using anti-mCgA-N′ showed CgA detection predominantly in neurons co-stained with anti-NeuN (**Fig. 5a**) and rarely in astrocytes labeled by antibody specific to glial fibrillary acidic protein (anti-GFAP; **Fig. 5b**). In contrast, prominent anti-mCgA-N′ immunoreactivity was observed in reactive astrocytes of ventral horn in presymptomatic G37R *SOD1* mice (**Fig. 5c–e**, 8 months old) and G93A *SOD1* mice (**Supplementary Fig. 5** online, 80 d old). CgA also localized in neurons (**Fig. 5c**) but not in Mac2-labeled microglia (**Fig. 5e**) of G37R *SOD1* mice. Pre-incubation with the peptide antigen completely eliminated the signal (data not shown). These results suggest that CgA may be involved in the disease progression concomitant with astrocytosis.

CgA and CgB promote secretion of mutant SOD1

The combined microscopy and immunoprecipitation data presented above provide compelling evidence for the selective colocalization of

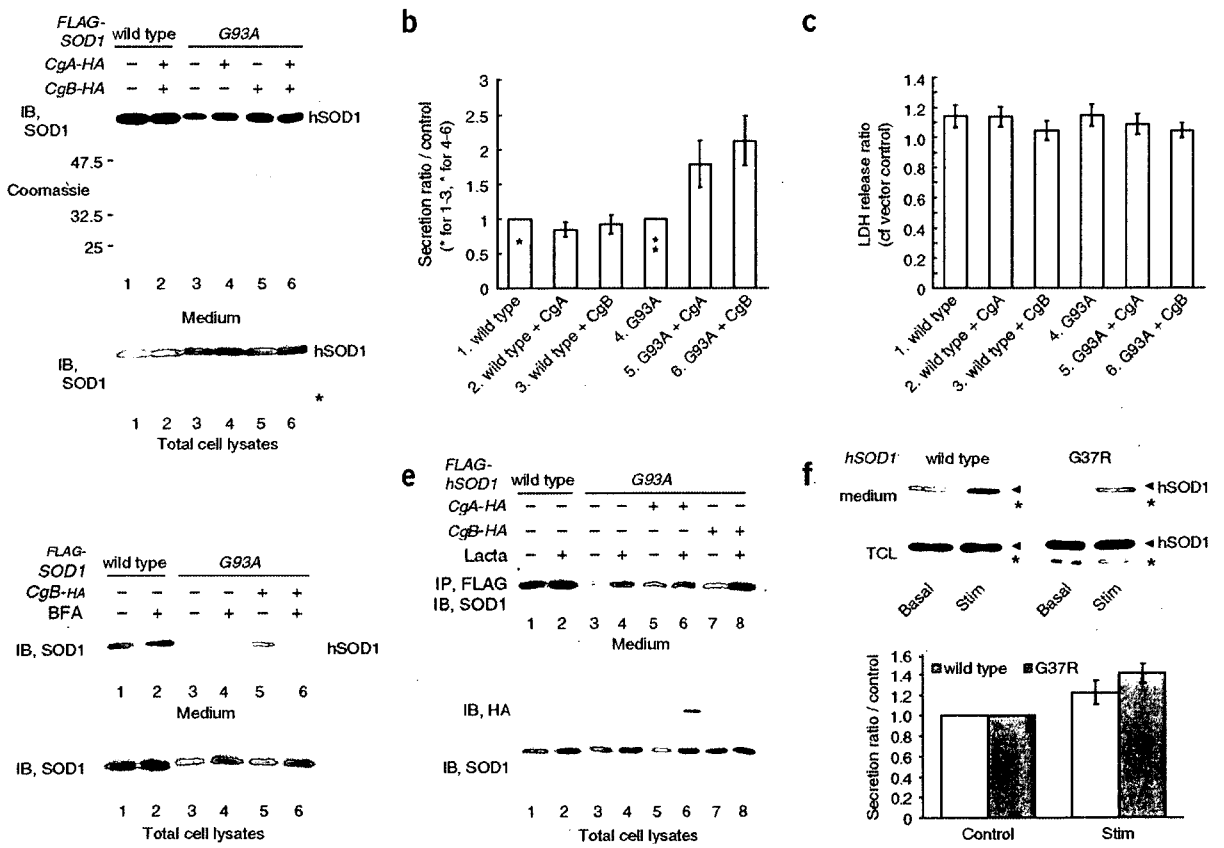

Figure 6 Chromogranins promote selective secretion of misfolded mutant SOD1. (**a**) CgA and CgB promoted specific secretion of mutant SOD1 in non-neurosecretory cells. COS-7 cells transfected with *FLAG-SOD1* (wild-type or G93A) and *CgA-HA* or *CgB-HA* were incubated in stimulation buffer. Medium was concentrated and analyzed by western blotting using SOD1-specific antibody. The SDS-PAGE gel was stained by Coomassie brilliant blue (Coomassie). Asterisk indicates endogenous SOD1. IB, immunoblot. (**b**) Densitometry of the secreted human SOD1 from the western blots. The values (mean ± s.e.m., $n = 3$) represent the ratio compared to control (lane 1 = control for wild-type (asterisk) and lane 4 = control for G93A SOD1 (double asterisks)). (**c**) LDH release assay demonstrating that transfection experiments did not provoke cell leakage. Medium was assayed 24 h after transfection. Value represents LDH release ratio compared with vector control (*pcDNA3*). Data are mean ± s.e.m. ($n = 3$). (**d**) Brefeldin A (BFA) inhibited chromogranin-mediated secretion of mutant SOD1. COS-7 cells transfected with FLAG-*SOD1* (wild-type or G93A) with or without CgB-HA were treated with 5 μM BFA for 1 h before exposure to stimulation buffer. (**e**) Effect of proteasomal inhibitor on mutant SOD1 secretion. Transfected NIH3T3 cells were treated with lactacystin for 20 h before the secretion assay. (**f**) Both wild-type and G37R SOD1 were secreted from embryonic spinal cord cultures from human SOD1 transgenic mice. Primary cultures were treated with basal or stimulation buffer for 15 min. Asterisks indicate endogenous mouse SOD1. Data given as ratio of secreted SOD1 from treated samples to that in basal-buffer samples (mean ± s.e.m., $n = 4$).

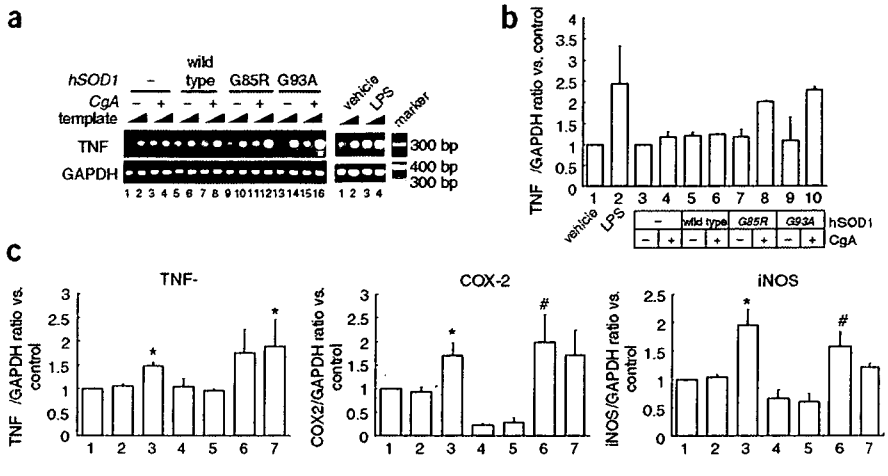

Figure 7 Activation of microglia by extracellular mutant SOD1. (**a**,**b**) Activation of microglial cell-line BV2 after treatment with conditioned medium from Neuro2a cells co-transfected with CgA and *SOD1* mutants (G85R or G93A). (**a**) RT-PCR study of TNF-α and GAPDH. For control, Neuro2a cells were treated with lipopolysaccharide (LPS). Notably, there was no microglial activation with medium from cells co-transfected with *CgA* and wild-type *SOD1*. Templates were examined at two different concentrations (1:10 diluted and original). (**b**) Each densitometric value was normalized with GAPDH and averaged from results of two different concentrations of templates. Each value represents a ratio compared to control lanes (bar 1 is the control for bar 2, and bar 3 is the control for 4–10), expressed as mean ± s.e.m. (**c**) Direct effect of mutant SOD1 on microglial activation. BV2 cells were treated with recombinant CgA (1 μg ml^{-1}), human SOD1 (wild-type or G93A, 2 μg ml^{-1} each) or LPS (10 μg ml^{-1}) as a positive control for 18 h, as shown in the bottom box. Semi-quantitative RT-PCR was performed in the same manner as in **a**. Each densitometric value was normalized by GAPDH and an expression ratio was obtained by comparison with control (bar 1 in each graph). The ratio was averaged from three experiments and expressed as mean ± s.e.m. *$P < 0.05$ versus sham treatment (lane 1). #$P < 0.05$ versus wild-type SOD1 treatment (lane 4) assessed by analysis of variance (ANOVA).

mutant SOD1 with chromogranins in mouse models of ALS. These results prompted us to investigate whether mutant SOD1 molecules were secreted together with chromogranins. We conducted secretion experiments using nongranular COS-7 cells that are lacking endogenous chromogranins[33]. Expression plasmids coding for FLAG-tagged SOD1 (wild-type or G93A mutant) and HA-tagged mouse CgA or CgB were transiently co-transfected in COS-7 cells. Both wild-type and G93A mutant SOD1 were detected by western analysis in the control medium after a 15-min incubation. Moreover, treatment with stimulation buffer containing 2-mM $BaCl_2$ and 50 mM KCl increased the amount of both wild-type and mutant SOD1 in the medium 1.2-fold compared with control buffer (data not shown). These data imply the existence of constitutive and regulatory secretory pathways for SOD1 in these cells. It is noteworthy that both CgA and CgB promoted secretion of G93A SOD1, whereas secretion of wild-type SOD1 was not affected by CgA or CgB (**Fig. 6a,b**). Judging from the amount of lactate dehydrogenase (LDH) released, the effects of chromogranins on secretion of mutant SOD1 did not result from cell death or membrane disintegration caused by overexpression (**Fig. 6c**). We also examined the effect of Brefeldin A (BFA) on SOD1 secretion to further address the involvement of the ER-Golgi network. In COS-7 cells, BFA did not reduce the secretion of either mutant or wild-type SOD1 in absence of CgB (**Fig. 6d**, lanes 2 and 5). BFA did, however, inhibit the CgB-mediated secretion of mutant SOD1 (**Fig. 6d**, lanes 7 and 8). This suggests that CgB contributes to the secretion of mutant SOD1 proteins through the TGN. We conclude that chromogranins promote the secretion of mutant SOD1, but not of wild-type SOD1.

Proteasome inhibition enhances secretion of mutant SOD1

Because previous studies showed an impairment of proteasomal activity in cells expressing mutant SOD1[11], we examined the effect of a proteasome inhibitor on the secretion of human SOD1 species in non-granular NIH3T3 cells. The treatment of transfected NIH3T3 cells with a specific proteasome inhibitor, lactacystin (5 μM), enhanced the secretion of mutant SOD1 in the presence or absence of chromogranins (**Fig. 6e**).

SOD1 secretion from spinal cultures of SOD1 mouse embryo

Both wild-type and mutant SOD1 have been detected in the cerebrospinal fluid (CSF) of *SOD1* transgenic rats[34] and humans carrying a SOD1 mutation[35]. However, it is technically difficult to prove this finding in mice, because of the small space for CSF with high occurrence of contamination from the blood or tissues. We carried out spinal cord cultures from *SOD1* transgenic mice to confirm that SOD1 can be secreted. Spinal cord cultures were prepared from E13 embryos and then analyzed after 14 d *in vitro*. Secretion analysis of the culture medium revealed that both wild-type and G37R SOD1 can be detected in basal secretion buffer. Exposure of the cells to stimulation buffer containing $BaCl_2$ (2 mM) and KCl (50 mM) for 15 min promoted the secretion of both wild-type and G37R SOD1, but more robustly in G37R (**Fig. 6f**). This result indicates that SOD1 can be secreted in both a constitutive and regulated manner.

Extracellular SOD1 mutants cause microgliosis and neuron death

There is evidence for involvement of CgA in microglial activation[32]. To examine the effects of secreted mutant SOD1 together with CgA on microglial activation, we treated BV2 microglial cells with conditioned medium from Neuro2a cells that were transfected with various human *SOD1* species (wild-type, G85R and G93A), with or without CgA. Semi-quantitative reverse-transcriptase PCR (RT-PCR) was performed using total RNA from BV2 cells to monitor expression of mRNA for proinflammatory molecules. RT-PCR results showed that the combination of mutant SOD1 and CgA resulted in a medium that induced TNF-α expression in BV2 cells (**Fig. 7a,b**).

To investigate whether extracellular SOD1 mutants activate microglia, we exposed the BV2 cells to recombinant human SOD1 or CgA (extracellular) to determine whether microglial activation was mediated directly by these molecules. The results showed that extracellular mutant G93A SOD1 with or without CgA induced BV2 cells to produce TNF-α, cyclooxygenase-2 (COX-2) and inducible nitric oxide synthase (iNOS) (**Fig. 7c**). In contrast to mutant SOD1, the recombinant wild-type SOD1 caused suppression of microglial activation, which is in agreement with a protective role for secreted wild-type SOD1 as recently suggested[35].

We further investigated the effects of extracellular SOD1 (wild-type and G93A) and CgA proteins using primary spinal cord cultures derived from E13 mouse embryos. Spinal cord cultures at 14 d after plating were exposed to these recombinant proteins or to lipopolysaccharide (LPS) for 24 h. Treatment of the cultures with CgA and/or

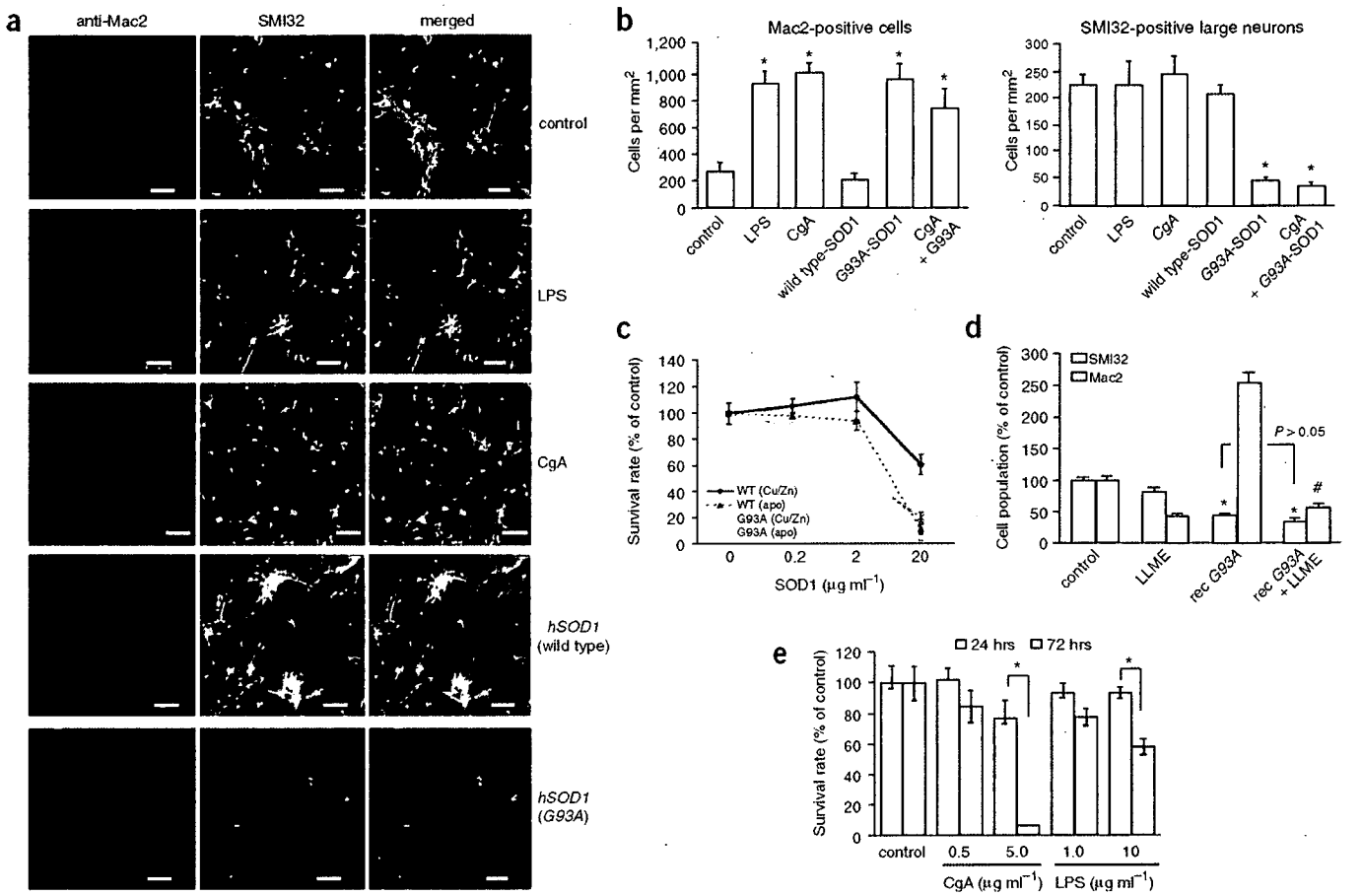

Figure 8 Extracellular SOD1 mutant triggers microgliosis and motor neuron death. (**a**) Immunofluorescence images of primary spinal cultures doubly stained by anti-Mac2 antibody and SMI32. Scale bars, 50 μm. (**b**) Extracellular SOD1 mutant activated microglia and killed motor neurons of embryonic spinal cord cultures. Spinal cord cultures were treated with lipopolysaccharide (LPS, 10 μg ml^{-1}), recombinant mouse CgA (5 μg ml^{-1}) or recombinant SOD1 (wild-type or G93A, 2 μg ml^{-1}) for 24 h. Cultures were fixed with 4% paraformaldehyde and doubly labeled with antibody to Mac2 (top) or antibody to the nonphosphorylated neurofilament NFH (SMI32) (bottom). The number of labeled cells at eight different areas from two sister cultures were averaged and expressed as cells per mm^2. Values indicate mean ± s.e.m. ($n = 8$). *$P < 0.01$ versus controls. (**c**) Dose-dependent toxicity of G93A and wild-type SOD1 in holo- or apo-states to spinal cord cultures. Spinal cultures were exposed to metal-deficient (apo) or metallated (Cu/Zn) recombinant G93A SOD1 or wild-type SOD1 for 24 h. Values indicate mean ± s.e.m. ($n = 8$). (**d**) Elimination of microglia did not affect extracellular SOD1-induced motor neuron death. Cultures were pre-treated with LLME (5 mM) for 16 h before application of recombinant G93A SOD1 (2 μg ml^{-1}) for 24 h. Values indicate percent survival compared with control culture (mean ± s.e.m., $n = 8$–24). *$P < 0.01$ versus control, #$P < 0.01$ versus recombinant G93A treatment. (**e**) Motor neuron death caused by longer time exposure to CgA. Spinal cultures were exposed to CgA or LPS for 72 h or 24 h. Values indicate mean ± s.e.m. ($n = 8$). *$P < 0.01$.

G93A SOD1 significantly increased the number of active microglia, like LPS treatment, as determined with antibody specific to Mac2 (**Fig. 8a** and top graph in **Fig. 8b**). On the other hand, whereas exposure to extracellular CgA (5 μg ml^{-1}) or LPS (10 μg ml^{-1}) for 24 h did not affect the number of motor neurons stained with SMI32 (an antibody that labels unphosphorylated neurofilament-H), recombinant SOD1 mutant (2 μg ml^{-1}) caused massive neuronal death (bottom row in **Fig. 8a** and bottom graph in **Fig. 8b**). Thus, both CgA and mutant SOD1 were capable of activating microglia, but only mutant SOD1 was neurotoxic after a 24-h exposure. This toxicity is not related to the metal content, as the apo G93A mutant also exhibited toxicity to motor neurons (**Fig. 8c**). Notably, the apo form of wild-type SOD1 acquired some toxicity at 20 μg ml^{-1} when compared to holo-state wild-type SOD1 (**Fig. 8c**). Furthermore, we investigated the role of microglia in extracellular mutant SOD1–induced motor neuron death by eliminating microglia with exposure to leu-leu methyl ester (LLME), a lysosomotropic agent that kills actively phagocytic cells such as microglia[36]. Treatment of spinal cultures with 5-mM LLME killed approximately 60–70% of Mac2-positive cells; control cultures showed only mild neurotoxicity (**Fig. 8d**). Pretreatment of the cell cultures with LLME did not rescue motor neurons from the toxicity of recombinant SOD1. Although these results indicate that extracellular SOD1 mutant can injure motor neurons independently of microglial activation, the role of microgliosis in motor neuron death cannot be excluded. The viability of motor neurons was affected by extracellular CgA or LPS after longer time exposures (**Fig. 8e**).

DISCUSSION

From the data presented here, we propose a novel pathogenic mechanism for ALS based on chromogranin-mediated secretion of misfolded SOD1 mutants (**Supplementary Fig. 6** online). This model is supported by the following findings: (i) chromogranins interact with ALS-linked SOD1 mutants but not with wild-type SOD1, (ii) chromogranins can promote selective secretion of mutant SOD1, (iii) mutant SOD1 is distributed in the TGN, (iv) extracellular mutant SOD1 can

trigger microgliosis and neuronal death and (v) CgA expression is induced in reactive astrocytes.

It is unclear how the mutant SOD1 proteins are being recruited in the ER-Golgi secretory granule pathway to interact with chromogranins. SOD1 protein has no signal sequence. It is possible that an increased hydrophobicity of mutant SOD1 underlies its translocation in the ER-Golgi pathway, as reported for fibroblast growth factor-16 (ref. 37). The cytosolic soluble protein SOD1 normally maintains its hydrophilicity through intramolecular disulfide bonds. However, mutant SOD1 proteins are readily monomerized by a reducing environment[38], resulting in exposure of hydrophobic regions that can be recognized by Hsp proteins[16]. Once recruited into the ER-Golgi system, it is plausible that oxidative conditions might promote the formation of oligomers, as detected in **Figure 3a**. Our findings are consistent with a previous report that mutant SOD1, but not wild-type SOD1, can induce ER stress when transfected into COS-7 cells, with accumulation of mutant SOD1 in or on the ER[39]. Although we cannot exclude the possibility of a gain of toxic function due to ER stress, our data demonstrate that secretion of mutant SOD1 may represent a toxic pathway which would be in line with the non-cell-autonomous nature of ALS[14].

It is still unclear how mutant SOD1 associates with chromogranins in the ER-Golgi network. The results from our yeast two-hybrid interaction studies support a direct association. Moreover, *in vitro* binding of recombinant CgA with mutant SOD1, but not with wild-type SOD1, was also confirmed (data not shown). The presence of Hsp70-like motifs in both CgB and CgA may explain why chromogranins interact with mutant forms of SOD1, but not with wild-type SOD1. Mutant SOD1 proteins are known to show altered solubility and interact with heat shock/stress proteins[15,16].

Previous studies have shown that wild-type SOD1 can be secreted from cultured astrocytes[40] or thymus-derived cells[41]. Moreover, it has been reported that both wild-type and mutant SOD1 species are detected in the cerebrospinal fluid of both transgenic rats[34] carrying human SOD1 and ALS patients with the SOD1 mutation[35]. Our data together with these observations support the idea that both wild-type and mutant SOD1 proteins may be secreted through non-classical secretory pathways[42]. In addition, we propose a chaperone-like function for chromogranins in mediating the selective secretion of misfolded SOD1 mutants through the ER-Golgi network. In a recent study[35] with NSC34 cells, the secretion was interpreted as being beneficial because the extrusion of mutant SOD1 attenuated formation of toxic intracellular inclusions, ameliorating cell survival. That study did not, however, consider the presence of glial cells in motor neuron environment *in vivo* or the possibility that the disease in not strictly cell autonomous[14]. Conversely, we posit that secretion of mutant SOD1 mediated by chromogranins is deleterious because extracellular mutant SOD1 proteins caused microgliosis and death of embryonic motor neurons in mixed cultures (**Fig. 8**). Unlike secreted mutant SOD1, extracellular wild-type SOD1 probably has protective properties. Our data suggest that extracellular wild-type SOD1 suppresses extracellular inflammation, perhaps through an antioxidant effect (**Fig. 7c**), which would be consistent with the finding that intraspinal infusion of exogenous wild-type SOD1 in G93A SOD1 transgenic rats prolonged their lifespan[34].

From our *in situ* hybridization data and immunohistochemistry of spinal cord samples, it seems that chromogranin expression is elevated in both motor neurons and interneurons (**Supplementary Fig. 2**). Therefore, as depicted in our proposed pathogenic scheme (**Supplementary Fig. 6**), we view interneurons as important contributors to the secretion of chromogranins and mutant SOD1 complexes in the vicinity of motor neurons. In this model, it is the burden of extracellular mutant SOD1 in close proximity to motor neurons that would increase the risk of damage. Even though interneurons and motor neurons themselves would be the predominant source of extracellular mutant SOD1 mediated by chromogranin interactions, mutant SOD1 secreted by other pathways from other cells such as microglia and astrocytes could also contribute to pathogenesis. Though the deleterious effects of intracellular mutant SOD1 can not be excluded, our model of toxicity based on secreted mutant SOD1 is compatible with the idea that the disease is not autonomous to motor neurons[14].

Although the exact mechanisms underlying the microgliosis and neurotoxicity of extracellular mutant SOD1 remain to be elucidated, various deleterious effects of misfolded SOD1 proteins may occur through generation of hydroxyl radicals[7], toxic oligomers[11] or amyloid-like filaments[43]. This model would support a linkage between inflammation and ALS pathogenesis[44,45]. Many factors may contribute to motor neuron death in the context of inflammation. Proinflammatory molecules such as TNF-α, Fas ligand or nitric oxide may act as mediators of motor neuron death[8]. Microglial activation alone is not usually sufficient to induce motor neuron death. For instance, induction of innate immunity by intraperitoneal injection of LPS does not injure motor neurons[44]. Chronic LPS administration precipitated ALS in mice, however, supporting the view that chronic inflammation may constitute a risk factor[44]. Yet, our data demonstrate that elimination of microglia by LLME did not alter survival of motor neurons and that LPS is much less toxic to motor neurons than mutant SOD1 in mixed embryonic spinal cord cultures (**Fig. 8b,e**). It is noteworthy that mutant SOD1, and to some extent wild-type SOD1, can be converted to toxic species even in absence of copper and zinc (**Fig. 8c**). This concurs with previous reports about the misfolded nature of apo-state SOD1 (refs. 16,43).

In conclusion, our results suggest a novel function for chromogranins in mediating the secretion of misfolded SOD1 mutants, a potentially toxic pathway that can induce inflammation and neuronal death. In future studies, it will be of interest to determine whether chromogranin-mediated secretion may be applicable to other neurodegenerative diseases that involve misfolded proteins.

METHODS

Materials. Commercially available antibodies are listed in **Supplementary Methods** online. The Golgi marker plasmid DsRed-Golgi, which carries the Golgi-targeting sequence of the human gene encoding β1,4-galactosyl transferase, was a generous gift from Y. Imai (RIKEN Brain Science Institute).

To generate an antibody specific to the N′ terminus of mouse CgA, we immunized rabbits with the peptide CLPVNSPMTKGDTKVMK, which encodes the amino terminal residues of mature mouse CgA (amino acids 18–35). The antisera were purified with an affinity column coupled with the same antigen. The titer and specificity were investigated by western blotting (**Supplementary Fig. 4**).

The recombinant proteins of human SOD1 (wild-type and mutant) and mouse CgA were generated from *Escherichia coli* as described in **Supplementary Methods.**

Transgenic mice. Transgenic mice harboring the G93A mutant of human *SOD1* (*B6SJL-TgN[SOD1-G93A]^{dl}1Gur, B6SJL-TgN[SOD1-G93A]1Gur*) and those harboring wild-type human *SOD1* (*C57Bl/6-TgN[SOD1]3Cje, hSOD1^{WT}*) were purchased from The Jackson Laboratory. Transgenic mice carrying G37R *SOD1* (line 29) were a kind gift from D. Cleveland (University of California, San Diego) and were housed and bred with C57Bl/6 mice. We selected these mouse lines because they were readily available to us. Since we maintain a larger colony of G37R *SOD1* (line 29) mice, most of our experiments involving mouse analysis were done with this line. Mice were treated with 10% chloral hydrate for anesthesia before they were perfused or killed. Animals were handled in accordance with the approved protocol by the animal experiment committees at RIKEN Brain Science Institute and by the Comité de Protection des Animaux de l'Université Laval.

Yeast two-hybrid screening. The plasmid *pGilda* carrying the G93A *SOD1* mutant was generated as bait for library screening. Yeast two-hybrid analysis (LexA/transactivation system) was performed on a cDNA library (1.5×10^6 independent clones) ligated into the *pJG4,5* plasmid from the total spinal cords of five preclinical transgenic mice carrying human G93A *SOD1* (*B6SJL-Tg(SOD1-G93A)1Gur/J*). Yeast two-hybrid screening was carried out using the Matchmaker Two-Hybrid System (Clontech) according to the manufacturer's protocol. There were 250 blue colonies that survived on the agar plates that contained galactose/raffinose and X-gal, but lacked tryptophan, histidine, leucine and uracil. All 250 were sequenced.

Plasmids, cell culture and transfection. Expression plasmids harboring human *SOD1* (wild-type, A4V, G85R or G93A) were prepared as reported previously[11]. The full-length murine genes encoding CgA (*Chga*) or CgB (*Chgb*) were cloned by RT-PCR using polyA-RNA from total brain of adult normal mice of the C57Bl/6 strain. See **Supplementary Methods** and **Supplementary Table 1** online for construction of EGFP-tagged CgB or deletion mutants of CgB. Cells from the murine neuroblastoma cell line Neuro2a, from the mouse fibroblast cell line NIH3T3 and COS-7 monkey ovary cells were maintained in nutrient medium containing 10% fetal bovine serum in the Dulbecco's minimal essential medium (DMEM, Sigma). The mouse microglial BV2 cells were cultured in DMEM-F12 Ham's (DF) medium containing 10% FBS. Cells were used for transfection using Lipofectamine Plus (Invitrogen) according to the manufacturer's protocol.

Immunoblotting and immunoprecipitation of cultured cells. Cells were lysed in TNT-G buffer consisting of 50 mM Tris-HCl (pH 7.4), 150 mM NaCl and 1% Triton-X100 with protease inhibitor cocktail (Roche) 24 h after the transfection. The cell lysates were incubated with anti-FLAG M2 agarose affinity gel (Sigma) for 1 h at 4 °C and were eluted with 4% SDS sample buffer. Samples were resolved by SDS-PAGE and transferred to a PVDF membrane (Polyscreen, PerkinElmer). A western blot image was obtained using a chemiluminescence detection kit (PerkinElmer).

Immunofluorescence and immunohistochemistry. Fixation of the cells and preparation of spinal cord slices is described in **Supplementary Methods**. After blocking, cultures or sections were incubated with primary antibodies and subsequently with corresponding fluorescent secondary antibodies (Alexa, Invitrogen) or with biotinylated secondary antibodies visualized by the avidin-biotin-immunoperoxidase complex (ABC) method using a Vectastain ABC kit (Vector Laboratories) and 3.3′-diaminobenzidine tetrahydrochloride (DAB; Sigma). The dilution rate of the primary antibodies is indicated in **Supplementary Methods**. Cells and tissue sections were observed by confocal laser microscopy (Olympus).

Subcellular fractionation of the spinal cord lysates. Spinal cord tissues from different ages of human *SOD1* transgenic mice were subcellularly fractionated into cytosolic, heavy and light membrane fractions, as described in **Supplementary Methods**. The protein concentration was determined by Bradford assay (BioRad), and an equal amount of protein was analyzed by western blotting. The percentage distribution of hSOD1 in post-nuclear fractions was also obtained by densitometric analysis and calculation of proportion from initial volume.

Sucrose-gradient ultracentrifugation of microsome fraction from spinal cord lysates. The light membrane (microsomal) fraction from spinal cord of *G37R SOD1* mice was further separated by sucrose gradient ultracentrifugation as previously described[46], with minor modifications that are decribed in **Supplementary Methods**. After overnight ultracentrifugation in sucrose cushions (5%, 30% and 40%), one-tenth (0.42 ml) was taken from the top of each sample, and the pellet was resuspended in MBS with 2 mM EDTA and 1% Triton-X100, and then concentrated using a centrifugal filter (Millipore) to 100 µl. Each fraction (20 µl) was separated by SDS-PAGE and analyzed by western blotting.

Immuno-isolation of TGN. To obtain pure preparations of TGN, we generated rabbit polyclonal antibody specific to the amino terminal peptides (CEGKRSKVTRRPKASDYQRLNLKL) of mouse/rat TGN38, a surface marker of TGN[47]. This anti-TGN38 or rabbit control IgG was bound to protein G-coated magnetic beads (Dynal) and was incubated with precleared post-mitochondrial fractions (described in more detail in **Supplementary Methods**). After washing, immunoprecipitates were eluted by 4% SDS sampling buffer and analyzed by western blotting with human SOD1-specific antibody (StressGen).

Immunoprecipitation of spinal cord lysates. The post-mitochondrial fractions of spinal cords were prepared by the same protocol as those in the immuno-isolation experiments. Rabbit polyclonal antibodies to CgA or CgB (Santa Cruz) or rabbit control IgG was bound to protein G-coated magnetic beads and incubated with precleared lysates, as described in **Supplementary Methods**. Immunoprecipitates were analyzed by Western blotting with human SOD1-specific antibody (StressGen).

Immunoelectron microscopy. We used post-embedding immunohistochemistry for electron microscopic observation, in which ultra-thin sections on the nickel grids were processed for immunohistochemistry without osmication. Fixation of the mice and preparation of ultrathin sections are described in **Supplementary Methods**. After blocking, grids were incubated with primary antibodies in the same buffer at 4 °C overnight, followed by a reaction with immunogold-conjugated secondary antibody (10 nm or 5 nm) for 1 h at 22 °C. For double staining, grids were further processed using another immunoreaction with a different primary and the secondary antibody with differently sized gold particles. Grids were observed by a TECNAI 12 electron microscope (FEI company).

Secretion assays. COS-7 and NIH3T3 cells were used in secretion experiments as non-neuronal cells lacking secretory granules[33]. At 24 h after transfection, cells plated onto a 6-well culture dish were washed in prewarmed PBS twice. Cells were incubated in basal secretion medium containing 10 mM HEPES, 129 mM NaCl, 5 mM $NaHCO_3$, 4.8 mM KCl, 1.2 mM $MgCl_2$, 1.2 mM KH_2PO_4, 1 mM $CaCl_2$ and 2.8 mM glucose (pH 7.4) for 1 h, and then treated with 1 ml of secretagogue-containing medium (stimulation buffer: 10 mM Hepes, 79 mM NaCl, 5 mM $NaHCO_3$, 50 mM KCl, 1.2 mM KH_2PO_4, 1.2 mM $MgCl_2$, 2 mM $BaCl_2$, 2.8 mM glucose, pH 7.4) for 15 min. In some experiments, Brefeldin A (BFA, 5 µM) was applied before exposure to stimulation medium. Lactacystin was applied in some assays 3 h after transfection and before incubation with basal buffer. We then collected 950 µl of medium and centrifuged it for 5 min at 1,000*g* to remove the debris. The supernatants were concentrated by a protein concentrator with 3.5 kDa cut-off (Millipore) to 60 µl, followed by western analysis. Secreted SOD1 was estimated by standardization with intracellular SOD1 in total cell lysates.

Primary cultures from embryonic spinal cord of transgenic mice carrying human *SOD1* (wild-type or *G37R*) were also investigated by secretion analysis. Cultures were prepared as explained below. Cell suspension from one spinal cord was plated onto one chamber in a six-well culture plate coated with polyethyleneimine. Secretion experiments were done after 14 d of culture *in vitro* using the protocol described above.

The content of LDH in the culture medium was measured in the medium 24 h after transfection using an LDH assay kit (Promega) according to the manufacture's protocol. Cells transfected with empty vector were used as a control.

Semi-quantitative reverse transcription PCR of microglial cell lines. Neuro2a cells were co-transfected with *pcDNA-SOD1* (wild-type, *G85R* or *G93A*) and *pcDNA3-CgA* in DF medium containing 10% FBS. At 16 h after transfection, the conditioned medium was transferred into the culture wells where BV2 cells had been previously plated, then further incubated for 24 h. Alternatively, BV2 cells were treated directly with recombinant proteins for 24 h. Then, cells were washed twice in PBS and total RNA was extracted using Trizol (Invitrogen). RT-PCR was conducted using oligo-dT primers according to the manufacturer's protocol (Invitrogen). The sequence of primer pairs is shown in **Supplementary Table 2** online. The gel images of PCR products obtained from illuminator were scanned, and densitometric analysis was performed using Scion image (Scion Corp.).

Primary culture of mouse embryonic spinal cord. Dissociated cultures of embryonic murine spinal cord were grown as previously described[11]. The spinal

cultures were treated at 11 or 14 d after plating. Motor neurons were identified as large cells labeled with SMI32 and active microglia were detected with Mac2-specific antibody. Confocal microscopy images were obtained from eight randomly selected fields, and immunoreactive cells were counted by computer. In several experiments, microglia were eliminated by a 16-h treatment with LLME[36] before exposure to recombinant SOD1 proteins. In preliminary experiments, we noticed that 5-mM LLME for 16 h killed approximately 60–70% of Mac2-positive cells. The number of cells was calculated as cells per mm^2 and averaged. Statistical significance was evaluated by single-factor ANOVA (analysis of variance) following Scheffe's method.

Note: Supplementary information is available on the Nature Neuroscience website.

ACKNOWLEDGMENTS

We thank R. Janvier for sample preparation for immunoelectron microscopy and B. Gentil for advice on experimental procedures. The technical help from G. Soucy, S.A. Ezzi (Laval University) and J. Kurisu (RIKEN Brain Science Institute) is appreciated. We thank D. Cleveland (University of California San Diego) for the G37R *SOD1* transgenic mice and Y. Imai for the *DsRed-Golgi* plasmid. This work was supported by the Canadian Institutes of Health Research (CIHR), the Robert Packard Centre for ALS Research at Johns Hopkins, the ALS Association (USA), the ALS Society of Canada, the Japan Society for the Promotion of Science (JSPS) and the Japan Foundation for Neuroscience and Mental Health. J.-P.J. holds a Canada Research Chair in Neurodegeneration. M.U. is a recipient of a Uehara Memorial Foundation research fellowship and a postdoctoral fellowship from CIHR.

COMPETING INTERESTS STATEMENT

The authors declare that they have no competing financial interests.

Published online at http://www.nature.com/natureneuroscience/
Reprints and permissions information is available online at http://npg.nature.com/reprintsandpermissions/

1. Rosen, D.R. *et al.* Mutations in Cu/Zn superoxide dismutase gene are associated with familial amyotrophic lateral sclerosis. *Nature* **362**, 59–62 (1993).
2. Gurney, M.E. *et al.* Motor neuron degeneration in mice that express a human Cu,Zn superoxide dismutase mutation. *Science* **264**, 1772–1775 (1994).
3. Subramaniam, J.R. *et al.* Mutant SOD1 causes motor neuron disease independent of copper chaperone-mediated copper loading. *Nat. Neurosci.* **5**, 301–307 (2002).
4. Wang, J., Xu, G. & Borchelt, D.R. High molecular weight complexes of mutant superoxide dismutase 1: age-dependent and tissue-specific accumulation. *Neurobiol. Dis.* **9**, 139–148 (2002).
5. Julien, J.P. Amyotrophic lateral sclerosis. unfolding the toxicity of the misfolded. *Cell* **104**, 581–591 (2001).
6. Cleveland, D.W. & Rothstein, J.D. From Charcot to Lou Gehrig: deciphering selective motor neuron death in ALS. *Nat. Rev. Neurosci.* **2**, 806–819 (2001).
7. Wiedau-Pazos, M. *et al.* Altered reactivity of superoxide dismutase in familial amyotrophic lateral sclerosis. *Science* **271**, 515–518 (1996).
8. Raoul, C. *et al.* Motoneuron death triggered by a specific pathway downstream of Fas: potentiation by ALS-linked SOD1 mutations. *Neuron* **35**, 1067–1083 (2002).
9. Durham, H.D., Roy, J., Dong, L. & Figlewicz, D.A. Aggregation of mutant Cu/Zn superoxide dismutase proteins in a culture model of ALS. *J. Neuropathol. Exp. Neurol.* **56**, 523–530 (1997).
10. Johnston, J.A., Dalton, M.J., Gurney, M.E. & Kopito, R.R. Formation of high molecular weight complexes of mutant Cu, Zn-superoxide dismutase in a mouse model for familial amyotrophic lateral sclerosis. *Proc. Natl. Acad. Sci. USA* **97**, 12571–12576 (2000).
11. Urushitani, M., Kurisu, J., Tsukita, K. & Takahashi, R. Proteasomal inhibition by misfolded mutant superoxide dismutase 1 induces selective motor neuron death in familial amyotrophic lateral sclerosis. *J. Neurochem.* **83**, 1030–1042 (2002).
12. Pramatarova, A., Laganière, J., Roussel, J., Brisebois, K. & Rouleau, G.A. Neuron-specific expression of mutant superoxide dismutase 1 in transgenic mice does not lead to motor impairment. *J. Neurosci.* **21**, 3369–3374 (2001).
13. Lino, M.M., Schneider, C. & Caroni, P. Accumulation of SOD1 mutants in postnatal motoneurons does not cause motoneuron pathology or motoneuron disease. *J. Neurosci.* **22**, 4825–4832 (2002).
14. Clement, A.M. *et al.* Wild-type nonneuronal cells extend survival of SOD1 mutant motor neurons in ALS mice. *Science* **302**, 113–117 (2003).
15. Shinder, G.A., Lacourse, M.C., Minotti, S. & Durham, H.D. Mutant Cu/Zn-superoxide dismutase proteins have altered solubility and interact with heat shock/stress proteins in models of amyotrophic lateral sclerosis. *J. Biol. Chem.* **276**, 12791–12796 (2001).
16. Urushitani, M. *et al.* CHIP promotes proteasomal degradation of familial ALS-linked mutant SOD1 by ubiquitinating Hsp/Hsc70. *J. Neurochem.* **90**, 231–244 (2004).
17. Taupenot, L., Harper, K.L. & O'Connor, D.T. The chromogranin-secretogranin family. *N. Engl. J. Med.* **348**, 1134–1149 (2003).
18. Rudolf, R., Salm, T., Rustom, A. & Gerdes, H.H. Dynamics of immature secretory granules: role of cytoskeletal elements during transport, cortical restriction, and f-actin-dependent tethering. *Mol. Biol. Cell* **12**, 1353–1365 (2001).
19. Li, J.Y., Leitner, B., Lovisetti-Scamihorn, P., Winkler, H. & Dahlström, A. Proteolytic processing, axonal transport and differential distribution of chromogranins A and B, and secretogranin II (secretoneurin) in rat sciatic nerve and spinal cord. *Eur. J. Neurosci.* **11**, 528–544 (1999).
20. Booj, S., Goldstein, M., Fischer-Colbrie, R. & Dahlstrom, A. Calcitonin gene-related peptide and chromogranin A: presence and intra-axonal transport in lumbar motor neurons in the rat, a comparison with synaptic vesicle antigens in immunohistochemical studies. *Neuroscience* **30**, 479–501 (1989).
21. Marksteiner, J. *et al.* Distribution of chromogranin B-like immunoreactivity in the human hippocampus and its changes in Alzheimer's disease. *Acta Neuropathol. (Berl.)* **100**, 205–212 (2000).
22. Rangon, C.M. *et al.* Different chromogranin immunoreactivity between prion and a-beta amyloid plaque. *Neuroreport* **14**, 755–758 (2003).
23. Schiffer, D., Cordera, S., Giordana, M.T., Attanasio, A. & Pezzulo, T. Synaptic vesicle proteins, synaptophysin and chromogranin A in amyotrophic lateral sclerosis. *J. Neurol. Sci.* **129** Suppl, 68–74 (1995).
24. Taupenot, L. *et al.* Chromogranin A triggers a phenotypic transformation and the generation of nitric oxide in brain microglial cells. *Neuroscience* **72**, 377–389 (1996).
25. Ciesielski-Treska, J. *et al.* Mechanisms underlying neuronal death induced by chromogranin A-activated microglia. *J. Biol. Chem.* **276**, 13113–13120 (2001).
26. Taylor, D.L., Diemel, L.T. & Pocock, J.M. Activation of microglial group III metabotropic glutamate receptors protects neurons against microglial neurotoxicity. *J. Neurosci.* **23**, 2150–2160 (2003).
27. Chanat, E., Weiss, U., Huttner, W.B. & Tooze, S.A. Reduction of the disulfide bond of chromogranin B (secretogranin I) in the trans-Golgi network causes its missorting to the constitutive secretory pathways. *EMBO J.* **12**, 2159–2168 (1993).
28. Cowley, D.J., Moore, Y.R., Darling, D.S., Joyce, P.B. & Gorr, S.U. N- and C-terminal domains direct cell type-specific sorting of chromogranin A to secretory granules. *J. Biol. Chem.* **275**, 7743–7748 (2000).
29. Li, J.Y., Kling-Petersen, A. & Dahlstrom, A. Influence of spinal cord transection on the presence and axonal transport of CGRP-, chromogranin A-, VIP-, synapsin I-, and synaptophysin-like immunoreactivities in rat motor nerve. *J. Neurobiol.* **23**, 1094–1110 (1992).
30. Kato, A. *et al.* Co-distribution patterns of chromogranin B-like immunoreactivity with chromogranin A and secretoneurin within the human brainstem. *Brain Res.* **852**, 444–452 (2000).
31. Stieber, A. *et al.* Disruption of the structure of the Golgi apparatus and the function of the secretory pathway by mutants G93A and G85R of Cu, Zn superoxide dismutase (SOD1) of familial amyotrophic lateral sclerosis. *J. Neurol. Sci.* **219**, 45–53 (2004).
32. Ciesielski-Treska, J. *et al.* Chromogranin A induces a neurotoxic phenotype in brain microglial cells. *J. Biol. Chem.* **273**, 14339–14346 (1998).
33. Huh, Y.H., Jeon, S.H. & Yoo, S.H. Chromogranin B-induced secretory granule biogenesis: comparison with the similar role of chromogranin A. *J. Biol. Chem.* **278**, 40581–40589 (2003).
34. Turner, B.J. *et al.* Impaired extracellular secretion of mutant superoxide dismutase 1 associates with neurotoxicity in familial amyotrophic lateral sclerosis. *J. Neurosci.* **25**, 108–117 (2005).
35. Jacobsson, J., Jonsson, P.A., Andersen, P.M., Forsgren, L. & Marklund, S.L. Superoxide dismutase in CSF from amyotrophic lateral sclerosis patients with and without CuZn-superoxide dismutase mutations. *Brain* **124**, 1461–1466 (2001).
36. Sharpless, N. *et al.* The restricted nature of HIV-1 tropism for cultured neural cells. *Virology* **191**, 813–825 (1992).
37. Miyakawa, K. & Imamura, T. Secretion of FGF-16 requires an uncleaved bipartite signal sequence. *J. Biol. Chem.* **278**, 35718–35724 (2003).
38. Tiwari, A. & Hayward, L.J. Familial amyotrophic lateral sclerosis mutants of copper/zinc superoxide dismutase are susceptible to disulfide reduction. *J. Biol. Chem.* **278**, 5984–5992 (2003).
39. Tobisawa, S. *et al.* Mutant SOD1 linked to familial amyotrophic lateral sclerosis, but not wild-type SOD1, induces ER stress in COS7 cells and transgenic mice. *Biochem. Biophys. Res. Commun.* **303**, 496–503 (2003).
40. Lafon-Cazal, M. *et al.* Proteomic analysis of astrocytic secretion in the mouse. Comparison with the cerebrospinal fluid proteome. *J. Biol. Chem.* **278**, 24438–24448 (2003).
41. Cimini, V. *et al.* CuZn-superoxide dismutase in human thymus: immunocytochemical localisation and secretion in thymus-derived epithelial and fibroblast cell lines. *Histochem. Cell Biol.* **118**, 163–169 (2002).
42. Nickel, W. The mystery of nonclassical protein secretion. A current view on cargo proteins and potential export routes. *Eur. J. Biochem.* **270**, 2109–2119 (2003).
43. Elam, J.S. *et al.* Amyloid-like filaments and water-filled nanotubes formed by SOD1 mutant proteins linked to familial ALS. *Nat. Struct. Biol.* **10**, 461–467 (2003).
44. Nguyen, M.D., D'Aigle, T., Gowing, G., Julien, J.P. & Rivest, S. Exacerbation of motor neuron disease by chronic stimulation of innate immunity in a mouse model of amyotrophic lateral sclerosis. *J. Neurosci.* **24**, 1340–1349 (2004).
45. Zhu, S. *et al.* Minocycline inhibits cytochrome c release and delays progression of amyotrophic lateral sclerosis in mice. *Nature* **417**, 74–78 (2002).
46. Parkin, E.T., Hussain, I., Karran, E.H., Turner, A.J. & Hooper, N.M. Characterization of detergent-insoluble complexes containing the familial Alzheimer's disease-associated presenilins. *J. Neurochem.* **72**, 1534–1543 (1999).
47. Stephens, D.J. & Banting, G. Direct interaction of the trans-Golgi network membrane protein, TGN38, with the F-actin binding protein, neurabin. *J. Biol. Chem.* **274**, 30080–30086 (1999).

The neuropeptide head activator is a high-affinity ligand for the orphan G-protein-coupled receptor GPR37

Meriem Rezgaoui[1], Ute Süsens[1], Atanas Ignatov[1], Mathias Gelderblom[2], Günter Glassmeier[3], Inga Franke[1], Jens Urny[1], Yuzuru Imai[4], Ryosuke Takahashi[4] and H. Chica Schaller[1,*]

[1]Zentrum für Molekulare Neurobiologie Hamburg, [2]Klinik und Poliklinik für Neurologie, and [3]Institut für Angewandte Physiologie, Universitätsklinikum Hamburg-Eppendorf, Martinistr. 52, 20246 Hamburg, Germany
[4]RIKEN Brain Science Institute, Saitama 351-0198, Japan
*Author for correspondence (e-mail: schaller@zmnh.uni-hamburg.de)

Accepted 26 October 2005
Journal of Cell Science 119, 542-549 Published by The Company of Biologists 2006
doi:10.1242/jcs.02766

Summary

The neuropeptide head activator (HA) is a mitogen for mammalian cell lines of neuronal or neuroendocrine origin. HA signalling is mediated by a G-protein-coupled receptor (GPCR). Orphan GPCRs with homology to peptide receptors were screened for HA interaction. Electrophysiological recordings in frog oocytes and in mammalian cell lines as well as Ca^{2+} mobilisation assays revealed nanomolar affinities of HA to GPR37. HA signal transduction through GPR37 was mediated by an inhibitory G protein and required Ca^{2+} influx through a channel of the transient receptor potential (TRP) family. It also required activation of Ca^{2+}-dependent calmodulin kinase and phosphoinositide 3-kinase. Respective inhibitors blocked HA signalling and HA-induced mitosis in GPR37-expressing cells. HA treatment resulted in internalisation of GPR37. Overexpression of GPR37 led to aggregate formation, retention of the receptor in the cytoplasm and low survival rates of transfected cells, confirming the notion that misfolded GPR37 contributes to cell death, as observed in Parkinson's disease.

Key words: G-protein-coupled receptor, GPR37, Head activator, Pael receptor, Parkinson, Signal transduction

Introduction

The undecapeptide head activator (HA) was originally isolated and characterised from hydra, where it mediates head-specific growth and differentiation processes, hence its name. In hydra, HA is produced by nerve cells and is stored in neurosecretory granules, from which it is released to initiate head regeneration and budding, and to maintain the normal head-to-foot morphology of hydra. At the cellular level, HA promotes proliferation of all cell types of hydra by acting as mitogen in the G2-mitosis transition; as for early mammalian development, this transition is the most important checkpoint to control cell-cycle progression. At higher concentrations, HA acts on the determination of stem cells to head-specific fates (Schaller et al., 1996).

HA was isolated with identical sequence from mammalian brain and intestine (Bodenmuller and Schaller, 1981). In adult mammals, HA enhances neurite outgrowth and is neuroprotective. HA is present during early mammalian development and is expressed in cells of the nervous and neuroendocrine system. Like in hydra, HA stimulates entry into mitosis and proliferation of cell lines derived from such origins. The signalling cascade from HA to mitosis includes activation of an inhibitory G protein and requires Ca^{2+} influx, downregulation of adenylyl cyclase and hyperpolarisation of the membrane potential (Kayser et al., 1998; Niemann and Schaller, 1996; Ulrich et al., 1996). For Ca^{2+} influx, a transient receptor potential (TRP)-like channel is responsible, which can be regulated by growth factors, such as insulin growth factor I (IGF-I) and platelet-derived growth factor (PDGF) (Kanzaki et al., 1999), and by HA (Boels et al., 2001). The increase in intracellular Ca^{2+} then triggers influx of K^+ through a Ca^{2+}-activated K^+ channel, leading to hyperpolarisation, which is an absolute requirement for entry into mitosis (Kayser et al., 1998).

In the search for receptors mediating the action of HA on stimulating mitosis in mammalian cells, we concentrated on orphan G-protein-coupled receptors (GPCRs) reacting with small peptides as ligands. GPCRs are the largest family of cell-surface receptors that mediate transduction of signals from the extracellular environment to intracellular effectors. They contain seven transmembrane domains and are activated by ligands of extremely different molecular origins and sizes including light, ions, metabolic intermediates, amino acids, nucleotides, lipids, peptides and proteins. These ligands primarily interact with the extracellular domains, but in part also with transmembrane regions of GPCRs. The classification of GPCRs into subfamilies is primarily based on their homology within the heptahelical structure (Frederiksson et al., 2003), but also on extracellular domains, and has been used to predict ligands for orphan receptors (Boels and Schaller, 2003; Ignatov et al., 2003a; Ignatov et al., 2003b). To find a receptor for HA, we concentrated on GPCR subfamilies reacting with small peptides as ligands.

Several orphan receptors failed to show interactions with HA, including GPR6 and GPR12, for which we found lysophospholipids as cognate ligands (Ignatov et al., 2003a;